Interactions between diet and gut microbiota and differentiated metabolic adaptations in sympatric migratory birds during autumn migration preparation at high altitudes

Yeying Wang[1]
Guizhou Normal University
Ai Wu[1]
Guizhou Normal University
Meng Fang[1]
Guizhou Normal University
Feng Jiang
jiangfeng@nwipb.cas.cn

Qinghai Provincial Key Laboratory of Qinghai-Tibet Plateau Biological Resources

Research Article

Keywords: high altitude, migratory birds, migration, gut microbiota, diet

Posted Date: August 14th, 2026

DOI: https://doi.org/10.21203/rs.3.rs-10456099/v1

Additional Declarations: No competing interests reported.

Abstract

To investigate food resource utilization and gut microbiota metabolic adaptation in sympatric migratory birds during autumn migration preparation at high altitudes (> 4,500 m), we studied *Grus nigricollis*, *Tadorna ferruginea*, and *Anser indicus* in the Yellow River Source Area of Sanjiangyuan National Park. Fecal DNA metabarcoding, 16S rRNA sequencing, Spearman correlation, and MetaCyc/KEGG pathway analyses revealed distinct interspecific differences in diet, gut microbiota, and metabolic functions. *G. nigricollis* preferred starch-rich *Argentina anserina* tubers and chitin-rich *Tipula subcunctans*, whereas *T. ferruginea* mainly consumed fiber-rich *Stuckenia pectinata* together with diverse animal foods, and *A. indicus* exhibited intermediate dietary diversity. The gut microbiota of *G. nigricollis* was dominated by lactic acid bacteria that fermented starch into short-chain fatty acids, promoting energy storage, while *T. ferruginea* was enriched in cellulolytic bacteria that converted fiber into energy. Although *A. indicus* exhibited the highest microbial diversity, no significant diet–microbiota correlation was detected. Functionally, *G. nigricollis* enhanced both catabolic and anabolic pathways for efficient fat accumulation, *T. ferruginea* primarily enriched anabolic pathways to support dietary diversity, and *A. indicus* optimized energy metabolism to maintain homeostasis. These findings provide new insights into microbial mechanisms underlying migratory energetics and inform wetland food resource management.

Introduction

Maduo County, located in Sanjiangyuan National Park, lies in the hinterland of the Qinghai-Tibet Plateau, with an average altitude exceeding 4,500 m. It is the source of the Yellow River and is known as the "China Water Tower". This region represents a typical alpine wetland ecosystem, characterized by low oxygen partial pressure, low annual mean temperature, and a short plant growing season, resulting in highly uneven spatiotemporal distribution of food resources. The area serves as an important breeding ground and migratory stopover site for several key protected migratory bird species in China, including the black-necked crane (*G. nigricollis*), ruddy shelduck (*T. ferruginea*), and bar-headed goose (*A. indicus*). In extreme environments above 4,500 m altitude, low oxygen, low temperature, and food scarcity constitute the main physiological constraints faced by animals(1). High altitude birds typically exhibit life history traits such as slower growth rates and prolonged nestling periods, but possess relatively higher body mass at fledging to enhance cold tolerance(2). Meanwhile, both bird species richness and individual abundance decrease significantly with increasing altitude(3). Therefore, exploring food adaptation strategies and energy metabolism regulation mechanisms in high altitude birds is of great ecological significance for elucidating species survival adaptation and migration completion mechanisms in extreme environments.

Previous studies have shown that the energy metabolism phenotype and gut microbiota composition of the Karoo thrush (*Cossypha caffra*) in South Africa are significantly correlated with environmental factors (such as climatic conditions and primary productivity) as well as genetic variation in genes related to energy metabolism. This suggests that the synergistic changes between selection pressure mediated by energy homeostasis regulatory genes and gut microbiota community structure may jointly drive the

adaptation of this species to extreme arid environments(4). Gut microbiota play a key role in host nutrient absorption, energy metabolism, and immune regulation, with diet considered the most important driver shaping gut microbiota structure and function(5, 6). Comparative studies based on sympatric coexisting species can effectively control for confounding effects of macroenvironmental variables, thereby enabling a more precise dissection of the relative contributions of host phylogenetic background and dietary composition to the formation of gut microbiota and their metabolic functions(7, 8). Existing research has preliminarily revealed the seasonal adaptation patterns of gut microbiota in high altitude birds. For example, in black necked cranes during the late wintering period (March), the gut is significantly enriched in Proteobacteria taxa associated with chitin, cellulose, and lipid degradation. Concurrently, fatty acid degradation and betalain biosynthesis pathways are significantly upregulated, indicating that they may expand their food spectrum, maintain gut fungal community stability, and improve food utilization efficiency to meet premigratory energy accumulation demands(9, 10). A year round study found that the gut microbial community structure of black necked cranes exhibits significant seasonal differentiation, with higher alpha and beta diversity in summer and dominance by Lactobacillaceae in other seasons. This dynamic change is closely linked to seasonal shifts in dietary composition(11). Furthermore, during altitudinal migration along the Gongga Mountain gradient, the gut microbiota of the Himalayan bluetail (*Tarsiger rufilatus*) can be markedly restructured within a short period (approximately one month), and a strong coupling relationship exists between animal based food intake and microbial community structure, further highlighting the dominant role of diet in driving dynamic changes in the gut microbiome(12).

However, systematic attention to the critical time window of the autumn migration preparation period remains insufficient, and there is a particular lack of integrated comparative studies on multiple sympatric migratory bird species under the same high-altitude extreme environment. In this study, we focus on sympatric foraging black-necked cranes, ruddy shelducks, and bar-headed geese in the Yellow River Source Area (Maduo County) of Sanjiangyuan National Park. During the autumn migration preparation period, we collected fecal samples and applied fecal DNA metabarcoding (using the mitochondrial *COI* gene to identify animal-based food sources and the chloroplast *rbcL* gene to identify plant-based food sources) and *16S rRNA* amplicon sequencing, combined with Spearman correlation analysis and metabolic pathway annotation and enrichment analysis (MetaCyc/KEGG), to carry out the following investigations: (1) In the context of the autumn migration preparation period, do sympatric black-necked cranes, ruddy shelducks, and bar-headed geese reduce interspecific food competition and achieve stable coexistence through trophic niche differentiation? Identify the plant and animal food resources that play key discriminating roles among the diets of the three bird species. (2) What are the gut microbiota community compositions and metabolic functional characteristics of the three bird species, and do their structure and function match their respective dietary traits? (3) Can the metabolic functional profile of the gut microbiota reflect the host's energy reserve and metabolic regulation strategies prior to long distance migration? From the multi-perspective of food composition and gut microbiota interactions, this study aims to reveal, for the first time, the migration preparation strategies of sympatric migratory birds under extreme environmental conditions in high altitude areas, providing

new scientific evidence for deepening the understanding of the mechanisms underlying host-gut microbiota interactions in ecological adaptation, and also offering theoretical support for the identification and scientific management of key food resources in the wetland ecosystem of Sanjiangyuan National Park.

Materials and methods

Sample collection

From September 23 to September 28, 2025, a total of 19 fecal samples were collected from black-necked cranes, 20 from ruddy shelducks, and 35 from bar-headed geese distributed in the core conservation area of Sanjiangyuan National Park, Madoi County, Qinghai Province (Fig. 1). To avoid disturbing the birds during foraging, sampling was conducted after the birds had finished feeding. A non-invasive method was used: fresh fecal samples were collected from the foraging grounds of the three bird species and placed into sterile fecal collection tubes. To prevent repeated sampling, the distance between any two fecal samples was maintained at more than 10 m. To avoid soil contamination, only the upper layer of each fecal sample was collected. The sampling tubes were immediately stored in a liquid nitrogen tank carried in the vehicle and subsequently transferred to a − 80 ℃ ultra-low temperature freezer in the laboratory.

Total DNA extraction, PCR amplification, and sequencing

Total genomic DNA was extracted from 0.5 g of each fecal sample using a fecal genomic DNA extraction kit (Tiangen Biotech Co., Ltd., Beijing, China) following the manufacturer's protocol, and DNA concentration and purity were quantified using a fluorescence-based assay (BioTek, Winooski, VT, USA). Because the freshness of fecal samples and their species origin (black-necked crane, ruddy shelduck, or bar-headed goose) could not be determined a priori, the primer pair mlCOIintF (5'-GGWACWGGWTGAACWGTWTAYCCYCC-3') and Fol-degen-rev (5'-TANACYTCNGGRTGNCCRAARAAYCA-3')(64, 65) was employed to simultaneously characterize animal-derived dietary components and identify host species. Based on sequence identification results, a total of 19 samples were assigned to black-necked crane (GN1–GN19), 20 samples to ruddy shelduck (TF1–TF20), and 35 samples to bar-headed goose (AI1–AI35) (Fig. 1). Plant-derived dietary components were analyzed using the chloroplast rbcL gene amplified with primers 3-F (5'-ATGTCACCACCAACAGAGACTAAAGC-3') and 3-R (5'-CGTCCTTTGTAACGATCAAG-3')(66, 67), while gut microbial communities were characterized by amplifying the V3-V4 region of bacterial 16S rRNA genes using universal primers 338F (5'-ACTCCTACGGGAGGCAGCAG-3') and 806R (5'-GGACTACHVGGGTWTCTAAT-3')(68). PCR amplification systems and cycling conditions followed previously published protocols(46). Amplified products were purified using the QIAquick Gel Extraction Kit (Qiagen, Hilden, Germany) and subsequently subjected to high-throughput sequencing on the Illumina MiSeq platform (Illumina, San Diego, CA, USA) by

Personalbio (Shanghai Personal Biotechnology Co., Ltd., Shanghai, China) in accordance with the manufacturer's instructions.

Data analysis

The standard operating procedure implemented in QIIME2(69) was used to identify and remove ambiguous or low-quality sequences. Since the DADA2 method(70) has not yet been adapted for *COI* and *rbcL* amplicons, it was applied only to the *16S rRNA* V3–V4 gene data for primer removal, quality filtering, and denoising, yielding a feature table (raw ASV table) and representative ASV sequences. Bacterial 16S rRNA gene sequences were taxonomically classified using the Greengenes database(71). For *COI* and *rbcL*, Vsearch(72) was used for read merging and chimera detection. The remaining high-quality sequences were then clustered into operational taxonomic units (OTUs) at a 97% sequence identity threshold(72). OTUs representing less than 0.001% of the total sequences across all samples were discarded. The *COI* and *rbcL* sequences were compared using BLAST searches against the NCBI nt database(73). Representative ASV or OTU sequences that could not be assigned to any known taxon were designated as "unclassified."

The standard workflow implemented in QIIME2(69) was employed for the identification and removal of ambiguous or low-quality sequences. As the DADA2 method(70) has not yet been optimized for *COI* and rbcL amplicons, it was applied exclusively to the *16S rRNA* V3–V4 region for primer trimming, quality filtering, and denoising, resulting in a feature table (raw ASV table) and corresponding representative ASV sequences. Taxonomic assignment of bacterial *16S rRNA* gene sequences was conducted using the Greengenes database(71). For *COI* and *rbcL* datasets, VSEARCH(72) was used for paired-end read merging and chimera detection. The retained high-quality sequences were subsequently clustered into operational taxonomic units (OTUs) at a 97% sequence identity threshold(72), and OTUs representing less than 0.001% of the total sequences across all samples were excluded to minimize spurious diversity. Taxonomic identification of *COI* and *rbcL* sequences was performed via BLAST searches against the NCBI nt database(73). Representative OTU sequences that could not be reliably assigned to any known taxon were classified as "unclassified."

To assess sequencing depth and adequacy, rarefaction curves were generated through random subsampling of sequences using QIIME2(69). Based on taxonomic annotations and the selected samples, dietary composition was characterized at the species level, whereas gut microbiota composition was profiled at the phylum, genus, and species levels.To comprehensively evaluate the richness and diversity of animal- and plant-based dietary components, as well as the gut microbial communities of the black-necked crane, ruddy shelduck, and bar-headed goose, six alpha diversity indices were calculated using QIIME2. These included the Chao1 index, Shannon index, Simpson index, observed species richness, Pielou's evenness index, and Good's coverage. Differences in alpha diversity among groups were assessed using the Kruskal–Wallis test, followed by Dunn's test for multiple pairwise comparisons, implemented in R (v4.1.3)(37). Statistically significant differences were visualized using boxplots. To further evaluate inter-sample variation, beta diversity analyses of both dietary

composition and gut microbiota were conducted based on Bray-Curtis distance. Group-level differences were tested using Analysis of Similarities (ANOSIM), and ordination was performed via principal coordinates analysis (PCoA)(74), with corrected P-values and 95% confidence intervals estimated using R packages (v4.1.3)(37).

To elucidate intrinsic patterns of co-occurrence and co-exclusion among microbial communities across the three bird species, ASV abundance data from all samples were utilized. Bray–Curtis distance was applied to construct hierarchical clustering trees using the average linkage method. The resulting dendrograms were integrated with bar plots to simultaneously visualize similarities in gut microbiota composition at the family level, both within and between groups. Following the assessment of community-level similarities and differences, LEfSe was employed to identify robust discriminatory taxa among animal-derived dietary components, plant-derived dietary components, and gut microbiota across the three bird species. A one-against-all (less stringent) comparison strategy was adopted, with group differences evaluated using the Wilcoxon test. The linear discriminant analysis (LDA) score threshold was set to 4 for all datasets. To further quantify associations between diet and microbiota, Spearman correlation coefficients were calculated between gut microbial taxa at the family level and selected animal- and plant-derived dietary components at the species level, applying a relative abundance threshold of > 1% across the three bird species. Functional potentials of bacterial communities, including metabolic and biosynthetic pathways, were predicted using the KEGG and MetaCyc databases via PICRUSt(75). Differentially abundant metabolic pathways were visualized using multifunctional bar plots. In addition, Spearman correlation analyses were conducted to assess relationships between significantly differential metabolic pathways and both dietary components at the species level (relative abundance > 1%) and gut microbiota at the family level. Group differences were further evaluated using the Wilcoxon rank-sum test.

All the above analyses were performed following the guide on the Genescloud Platform of Personalbio, a free online platform for data analysis (https://www.genescloud.cn).

Results

Sequencing analysis

High-throughput sequencing on the Illumina MiSeq platform generated 5,971,316 high-quality, non-chimeric *COI* sequences, 7,593,467 *rbcL* sequences, and 3,862,299 sequences for the V3–V4 region of bacterial 16S rRNA (Supplementary Table S1); rarefaction curves based on the Shannon index for *COI*, *rbc*L, and *16S rRNA* datasets demonstrated that sequencing depth approached saturation across all samples, indicating sufficient coverage to reliably characterize both dietary and microbial communities (Supplementary Fig. S1). Based on the top 20 taxa by relative abundance, *COI*-derived dietary components in the black-necked crane, ruddy shelduck, and bar-headed goose comprised 6, 9, and 9 phyla; 6, 10, and 9 classes; 8, 13, and 11 orders; 8, 14, and 12 families; 8, 15, and 12 genera; and 9, 15, and 14 species, respectively, whereas plant-derived components identified via rbcL exhibited a

consistent taxonomic profile across species, encompassing 1 phylum, 1 class, 9 orders, 11 families, 19 genera, and 20 species. The gut microbiota of the three bird species comprised 6, 7, and 7 phyla; 8, 9, and 9 classes; 9, 11, and 12 orders; 13, 17, and 18 families; 14, 18, and 19 genera; and 15, 18, and 20 species, respectively. Given that taxonomic resolution and assignment rates were highest at the species level, all subsequent analyses were conducted at the species level or higher taxonomic ranks.

Analysis of dietary composition and diversity of Black-necked Cranes, Ruddy Shelducks, and Bar-headed Geese

Based on mitochondrial *COI* and *rbcL* gene sequencing, the dietary composition and plant-derived components of the black-necked crane (group GN), ruddy shelduck (group TF), and bar-headed goose (group AI) were systematically characterized. At the species level, considering only taxa with reliable identification rates (> 85% for *COI* and > 95% for *rbcL*) and relative abundances exceeding 1%, *COI*-based analyses (Fig. 2a) revealed that the GN group contained a single dominant dietary item, *T. subcunctans* (78.21%); the TF group comprised ten taxa, including *Chlorella* sp. (10.09%), *Marrus orthocanna* (4.73%), *Hydrodictyon reticulatum* (6.77%), *Syllepte* sp. (10.09%), *Kurtiella bidentata* (18.47%), *Drosophila eugracilis* (4.99%), *Boletina trispinosa* (1.88%), *Limnodrilus claparedianus* (3.52%), *Pterochondria woodii* (1.15%), and *Chironomus circumdatus* (1.84%); and the AI group included fifteen taxa, namely *T. subcunctans* (3.08%), *Chlorella* sp. (5.96%), *Thalassia hemprichii* (9.81%), *M. orthocanna* (4.89%), *B. trispinosa* (2.33%), *Mallodon dasystomus* (3.68%), *P. woodii* (2.77%), *Herposiphonia tenella* (2.39%), *Lecane lunaris* (1.84%), *Emballonura alecto* (2.28%), *Elaeis guineensis* (2.28%), *Euphyllia* sp. (1.56%), *Culex bahamensis* (1.46%), *Cordyla* sp. (1.56%), and *Carabus violaceus* (1.04%). In addition, COI data suggested potential parasitic infections, including *Eimeria gruis* (7.10%) in GN, *Isospora cf. erithaci* (12.41%) and *Eimeria* sp. (1.46%) in TF, and *Eimeria* sp. (8.42%) and *Eimeria nocens* (4.37%) in AI (Fig. 2a). Fungal taxa such as *Penicillium chrysogenum*, *Filobasidium floriforme*, *Lichtheimia* sp., and *Melampsora magnusiana* were also detected (Fig. 2a), which may reflect incidental ingestion or widespread environmental occurrence. Several bacterial taxa commonly associated with environmental substrates, plant surfaces, or gut microbiota-including *Escherichia coli*, *Klebsiella pneumoniae*, *Rhizobium leguminosarum*, and *Sphingomonas* sp. (Fig. 2a) were identified; these non-dietary components were excluded from subsequent analyses. Plant-parasitic nematodes, such as *Meloidogyne graminicola* and *Bursaphelenchus cocophilus*, were likely introduced via plant consumption. Analysis of *rbcL* sequences (Fig. 2b) indicated that plant-derived dietary components with relative abundances > 1% included six species in GN (*S. pectinata* 22.31%, *A. anserina* 52.30%, *Carex hystericina* 13.59%, *Fallopia convolvulus* 1.73%, *Triglochin palustris* 2.80%, and *Lysimachia maritima* 1.03%), five species in TF (*S. pectinata* 63.55%, *C. hystericina* 1.09%, *Laccopetalum giganteum* 24.43%, *Myriophyllum aquaticum* 3.31%, and *Taraxacum platypecidium* 3.00%), and seven species in AI (*S. pectinata* 36.49%, *A. anserina* 9.56%, *C. hystericina* 16.47%, *Puccinellia distans* 23.75%, *F. convolvulus* 4.85%, *T. palustris* 1.08%, and *Chrysopogon zizanioides* 3.32%) (Fig. 2b).

Alpha diversity metrics were calculated for dietary components to compare differences among the three groups (TF, AI, GN). For COI-derived animal dietary data, the Chao1 index ($P < 0.05$), Simpson index ($P < 0.01$), Shannon index ($P < 0.01$), and observed species richness ($P < 0.05$) were significantly higher in

group TF than in group GN, whereas no significant differences were detected between group TF and group AI for these indices, and no other alpha diversity metrics showed statistically significant variation among groups (Fig. 2c). For *rbcL*-derived plant dietary data, both the Chao1 index and observed species richness ($P < 0.001$) were significantly lower in groups AI and TF compared with group GN, indicating reduced plant dietary richness in the former two groups; in contrast, the Good's coverage showed highly significant differences ($P < 0.001$), with significantly higher values in groups TF and AI than in group GN, and TF also significantly exceeding AI, suggesting improved sampling completeness in these groups. Additionally, the Shannon index was significantly lower only in group TF compared with group GN ($P < 0.05$), while no significant difference was observed between groups AI and GN (Fig. 2d). Collectively, these results indicate that, for plant-based dietary components, group GN exhibited significantly higher species richness (Chao1 and observed species) than both TF and AI, as well as higher Shannon diversity than TF; conversely, group GN showed significantly lower Good's coverage than TF and AI, representing the lowest sequencing coverage among the three groups.

To further investigate differences in dietary composition among groups, Principal Coordinates Analysis (PCoA) and Analysis of Similarities (ANOSIM) were conducted. The ANOSIM results indicated that all pairwise comparisons yielded $R > 0$ (Fig. 2e), suggesting that intergroup variation exceeded intragroup variation. Analysis of COI sequence data revealed significant differences ($P < 0.05$) among all pairwise comparisons (GN vs. TF, GN vs. AI, and TF vs. AI) (Fig. 2e). Similarly, the *rbcL* sequence data exhibited comparable patterns, showing consistent and significant separation among groups (Fig. 2f).

To identify significantly differentiated dietary components among groups, a comparative analysis was conducted using LEfSe with an LDA score threshold set at 4. Based on *COI* sequencing results, the GN group was characterized by a significant enrichment of *T. subcunctans* (Diptera, Tipulidae) relative to the other groups. The TF group showed significant enrichment of multiple taxa, including *K. bidentata* (Bivalvia, Venerida, Montacutidae), *Chlorella* sp. (Trebouxiophyceae, Chlorellales, Chlorellaceae), *H. reticulatum* (Chlorophyceae, Sphaeropleales, Hydrodictyaceae), *D. eugracilis* (Diptera, Drosophilidae), and *Ranunculus carolinianus* (Ranunculaceae). In contrast, the AI group was primarily characterized by significantly enriched taxa belonging to Mycetophilidae and Culicidae (Fig. 3a). For *rbcL*-derived plant dietary data, the GN group exhibited significant enrichment of Rosales at the order level and *A. anserina* at the species level compared with the other two groups. In the TF group, significantly differentiated taxa included Potamogetonaceae at the family level, as well as *S. pectinata*, Alismatales, Ranunculaceae, Ranunculales, Asteraceae, Asterales, and *T. platypecidium*. In the AI group, *P. distans* (Poales, Poaceae) and *C. hystericina* (Poales, Cyperaceae) were identified as significantly differentiated taxa relative to the other groups (Fig. 3b).

Analysis of gut microbiota composition and diversity in Black-necked Cranes, Ruddy Shelduck, and Bar-headed Geese

The gut microbiota composition of the black-necked crane, ruddy shelduck, and bar-headed goose was characterized using 16S rRNA gene sequencing. At the phylum level, seven taxa with mean relative abundances exceeding 1% displayed distinct compositional patterns among the GN, TF, and AI groups. The relative abundances of Firmicutes_D were 70.13%, 25.23%, and 23.10%; Actinobacteriota were 9.64%, 33.18%, and 30.63%; Proteobacteria were 7.45%, 10.74%, and 13.33%; and Bacteroidota were 1.96%, 9.02%, and 9.30% in the GN, TF, and AI groups, respectively. In addition, Firmicutes_A (15.25% and 18.80%) and Chloroflexota (1.69% and 3.38%) were detected in the TF and AI groups, whereas Fusobacteriota (9.46%) was uniquely enriched in the GN group; these three phyla were present at relative abundances below 1% in the remaining groups (Fig. 4a). At the genus level, six genera in the GN group exhibited relative abundances greater than 1%, including *Ligilactobacillus* (45.15%), *Carnobacterium* (12.54%), *Cetobacterium* (9.46%), *Catellicoccus* (6.46%), *Serratia* (4.46%), and *Liquorilactobacillus* (2.98%). In the TF group, 11 genera exceeded 1% relative abundance, including *Ligilactobacillus* (11.91%), *Carnobacterium* (1.03%), *Actinotalea* (4.81%), *Planococcus* (3.72%), *Romboutsia* (1.01%), *Clostridium* (2.75%), *Ilumatobacter* (1.90%), *Streptococcus* (1.69%), *Acinetobacter* (2.13%), *Thermophilibacter* (2.45%), and *Adlercreutzia* (1.97%). In the AI group, 18 genera were identified with relative abundances exceeding 1%, including *Ligilactobacillus* (4.87%), *Carnobacterium* (1.22%), *Actinotalea* (3.51%), *Planococcus* (2.92%), *Enterococcus* (4.55%), *Terrisporobacter* (3.89%), *Acetobacterium* (3.89%), *Romboutsia* (3.02%), *Clostridium* (1.10%), *Ilumatobacter* (1.45%), *Streptococcus* (1.90%), *Aquipuribacter* (3.12%), *Arthrobacter* (2.55%), *Rothia* (2.35%), *Exiguobacterium* (1.54%), *Turicibacter* (1.64%), *Pseudomonas* (1.14%), and *Paracoccus* (1.15%) (Fig. 4b). At the species level, although overall detection frequencies were lower, several taxa with relative abundances exceeding 1% were still identified. In the GN group, *Carnobacterium maltaromaticum* (8.25%), *Cetobacterium somerae* (8.49%), and *Catellicoccus marimammalium* (4.73%) were detected. The TF group contained *Thermophilibacter avicola* (2.44%), *Streptococcus parasuis* (1.26%), and *Acinetobacter harbinensis* (1.23%). In the AI group, the detected species included *Romboutsia bilealis* (2.99%), *Enterococcus cecorum* (4.53%), *Aquipuribacter hungaricus* (3.04%), *Arthrobacter flavus* (1.24%), and *Turicibacter sanguinis* (1.63%) (Fig. 4c).

Alpha diversity indices, including the Simpson index, Shannon index, and observed species richness, were calculated to compare gut microbiota diversity among the three groups (Fig. 4d). All three indices exhibited higher values in group AI than in group GN, indicating an overall increase in microbial diversity in AI. In addition, group AI also showed higher alpha diversity than group TF, and group TF displayed higher values than group GN; however, these intergroup differences did not reach statistical significance.

To further evaluate differences in gut microbiota composition among groups, Principal Coordinates Analysis (PCoA) and Analysis of Similarities (ANOSIM) were performed (Fig. 4e). The ANOSIM results indicated that pairwise comparisons between the GN and AI groups, as well as between the TF and AI groups, yielded R values greater than 0, suggesting that intergroup variation exceeded intragroup variation. Notably, significant differences were detected among all pairwise comparisons, including GN vs. AI, GN vs. TF, and TF vs. AI ($P < 0.05$), indicating distinct gut microbial community structures among the three bird species.

To characterize similarities and differences in gut microbiota composition both within and between groups, hierarchical clustering analysis was conducted and the results were visualized using an interactive bar plot (Fig. 5a). The AI (*A. indicus*) and TF (*T. ferruginea*) samples exhibited a high degree of compositional similarity and were predominantly clustered together, whereas a subset of AI samples (AI6-AI9) clustered with the GN group, indicating partial overlap in microbial community structure between these groups.

To identify gut microbial taxa exhibiting significant differences both between and within groups, a comparative analysis was conducted using LEfSe with an LDA score threshold set at 4. In the gut microbiota of black-necked cranes, three microbial species—*C. marimammalium* (Bacilli, Lactobacillales, Catellicoccaceae), *C. somerae* (Fusobacteriota, Fusobacteriia, Fusobacteriales, Fusobacteriaceae), and *Carnobacterium gallinarum* (Bacilli, Lactobacillales, Carnobacteriaceae) together with six genera (*Ligilactobacillus*, *Carnobacterium*, *Cetobacterium*, *Catellicoccus*, *Serratia*, and *Liquorilactobacillus*), were significantly differentiated compared with those of ruddy shelducks (*T. ferruginea*) and bar-headed geese (*A. indicus*). In ruddy shelducks, four genera (*Planococcus*, *Actinotalea*, *Clostridium*, and *Adlercreutzia*) were identified as significantly different relative to the other two groups. In bar-headed geese, one species (*E. cecorum*, Enterococcaceae) and four genera (*Terrisporobacter*, *Acetobacterium*, *Arthrobacter*, and *Rothia*) exhibited significant differentiation in gut microbiota composition compared with the other groups (Fig. 5b).

- *Interactions of plant-based and animal-based foods with gut microbiota and predictive functional analysis of gut microbes*

Spearman correlation analysis was performed to assess the relationships between the relative abundances of gut microbial taxa and the plant- and animal-derived dietary components of black-necked cranes, ruddy shelducks, and bar-headed geese. In group GN (Fig. 6a), plant-derived dietary components with relative abundances exceeding 1% were significantly associated with 10 gut microbial taxa also present at > 1% relative abundance. The occurrence of *L. maritima* and *T. palustris* showed significant positive correlations with members of Marinilabiliaceae, Beutenbergiaceae, Dermatophilaceae, Peptostreptococcaceae, and Planococcaceae. In addition, *L. maritima* was significantly positively correlated with Nocardioidaceae, Propionibacteriaceae, Rhodobacteraceae, Rhizobiaceae, and Ilumatobacteraceae. No significant associations were detected between other plant-derived dietary components and gut microbial taxa, and no significant negative correlations were observed. Regarding the animal-derived diet of black-necked cranes, only *T. subcunctans* was detected, precluding correlation analysis due to the absence of multiple dietary variables. In group TF, *S. pectinata* exhibited significant positive correlations with Cellulomonadaceae, Nocardioidaceae, and Eubacteriaceae; *L. giganteum* showed significant positive correlations with Marinilabiliaceae and Fusobacteriaceae, and a significant negative correlation with Cellulomonadaceae; and *T. platypecidium* was significantly positively correlated with Cellulomonadaceae (Fig. 6b). In the analysis of animal-derived dietary components, Clostridiaceae was significantly positively correlated with both *Syllepte* sp. and *B. trispinosa*, while Eubacteriaceae showed a significant positive correlation with *B. trispinosa* (Fig. 6c). In group AI, no significant

correlations were detected between either plant- or animal-derived dietary components and gut microbiota composition in bar-headed geese.

This study performed functional enrichment analysis of secondary metabolic pathways using the MetaCyc and visualized the results using differential boxplots. A total of 14 significantly differentiated secondary metabolic pathways were identified (Fig. 6d), with distinct enrichment patterns observed among the three groups. The GN group showed significant enrichment in Carboxylate Degradation, Glycolysis, Carbohydrate Degradation, Cell Structure Biosynthesis, Fatty Acid and Lipid Biosynthesis, and Nucleoside and Nucleotide Biosynthesis (Fig. 6d). Overall, the GN group exhibited enrichment in both biosynthetic and degradative pathways, suggesting that black-necked cranes efficiently utilize carbon sources for catabolic energy production while simultaneously maintaining active biosynthesis of cellular structures and macromolecules, indicative of a highly metabolically active state. The TF group was significantly enriched in Aromatic Compound Biosynthesis, Cell Structure Biosynthesis, Fatty Acid and Lipid Biosynthesis, and Amino Acid Biosynthesis, with enrichment predominantly concentrated in anabolic pathways, indicating that ruddy shelducks primarily allocate metabolic activity toward the synthesis of secondary metabolites and structural components. The AI group showed significant enrichment in C1 Compound Utilization and Assimilation, Inorganic Nutrient Metabolism, Electron Transfer, Nucleoside and Nucleotide Degradation, and Cofactor, Prosthetic Group, Electron Carrier, and Vitamin Biosynthesis, suggesting a metabolic strategy biased toward energy metabolism, electron transport processes, and cofactor biosynthesis, while maintaining metabolic balance through nucleotide degradation. Notably, except for Nucleoside and Nucleotide Degradation, no significant differences in pathway enrichment were observed between the TF and AI groups.

During KEGG pathway analysis, a total of 17 significantly differentiated secondary pathways were identified (Fig. 6e). Compared with the AI and TF groups, the GN group exhibited significant enrichment in Cell growth and death, Nucleotide metabolism, Membrane transport, Glycan biosynthesis and metabolism, Translation, Replication and repair, Lipid metabolism, Metabolism of other amino acids, and Carbohydrate metabolism. In contrast, relative to the GN group, the TF group showed significant enrichment in Transcription and Energy metabolism, whereas the AI group demonstrated significant enrichment in Transport and catabolism, Signal transduction, Cell motility, Biosynthesis of other secondary metabolites, Lipid metabolism, Metabolism of cofactors and vitamins, and Amino acid metabolism. Between the TF and AI groups, significant differences were observed only in Cell growth and death, Translation, and Carbohydrate metabolism, with no significant differences detected in the remaining pathways (Fig. 6e), indicating that TF and AI share broadly similar overall metabolic profiles, although the TF group may exhibit slightly higher or functionally distinct activity in growth- and translation-related processes compared with the AI group. These results are generally consistent with the predictions based on MetaCyc analysis, suggesting that the GN group is characterized by an overall high metabolic activity state, particularly with pronounced enrichment in energy substance biosynthesis, cellular proliferation, and macromolecular synthesis pathways, features typically associated with rapidly growing and actively proliferating cells or tissues. Compared with the GN group, the TF group appears to rely more on transcriptional regulation and modulation of energy metabolism. In contrast, the AI group is

characterized by stronger environmental responsiveness, enhanced catabolic activity, and increased synthesis of specialized metabolites, suggesting a metabolic state dominated by regulatory flexibility and metabolic reprogramming rather than large-scale biosynthesis.

Spearman correlation analysis was conducted to examine the associations between significantly differentiated metabolic pathways (identified through MetaCyc and KEGG) and dietary components (animal- and plant-derived) with relative abundances exceeding 1% across the three groups. For animal- and plant-derived dietary components, significant correlations were detected only in group TF. Specifically, amino acid metabolism showed significant negative correlations with *Chlorella* sp. (10.09%), *H. reticulatum* (6.77%), and *B. trispinosa* (1.88%). In contrast, glycolysis exhibited significant positive correlations with *Chlorella* sp., *H. reticulatum*, and *D. eugracilis*, while showing a significant negative correlation with *L. claparedianus* (Fig. 7a). For plant-derived dietary components, significant correlations were observed only in group GN, where *S. pectinata* (22.31%) was significantly negatively correlated with carbohydrate metabolism, and both *T. palustris* (2.80%) and *L. maritima* (1.03%) were significantly negatively correlated with membrane transport (Fig. 7b); no comparable correlations were detected in the other groups. In addition, Spearman correlation analyses were performed between gut microbial taxa (relative abundance > 1%) and significantly differentiated functional pathways across the three groups. The results showed that gut microbiota were broadly associated with functional pathways in all groups, exhibiting significant positive correlations, significant negative correlations, as well as a small proportion of non-significant associations (Fig.s 7c, 7d, and 7e). Collectively, these findings suggest that gut microbiota exert a more pronounced influence on functional metabolic pathways than dietary components in shaping functional profiles.

Spearman correlation analysis was conducted to examine the relationships between significantly differentiated metabolic pathways (as identified by MetaCyc and KEGG analyses) and dietary components of animal- and plant-derived origin with relative abundances exceeding 1% in each of the three groups. The results indicated that, for animal-derived dietary components, significant correlations were observed only in group TF: amino acid metabolism exhibited significant negative correlations with *Chlorella* sp. (10.09%), *H. reticulatum* (6.77%), and *B. trispinosa* (1.88%), whereas glycolysis showed significant positive correlations with *Chlorella* sp., *H. reticulatum*, and *D. eugracilis*, but a significant negative correlation with *L. claparedianus* (Fig. 7a). For plant-derived dietary components, significant correlations were detected only in group GN: *S. pectinata* (22.31%) was significantly negatively correlated with carbohydrate metabolism, while *T. palustris* (2.80%) and *L. maritima* (1.03%) were significantly negatively correlated with membrane transport (Fig. 7b); no comparable correlations were observed in the other groups. In addition, Spearman correlation analysis was further applied to evaluate associations between gut microbial taxa (relative abundance > 1%) and significantly differentiated functional pathways across groups. The results showed that, across all three groups, gut microbial taxa were consistently linked to functional pathways, exhibiting either significant positive or negative correlations, while only a limited number of associations were non-significant (Fig.s 7c, 7d, and 7e). These findings suggest that gut microbiota exert a stronger influence on functional pathway variation than dietary

composition, indicating that microbial community structure plays a more dominant role in shaping functional potential than food source alone.

Disscution

Analysis of Food Composition of Sympatric Foraging Black-necked Cranes, Ruddy Shelducks, and Bar-headed Geese during the Autumn Migration Preparation Period

To investigate the food preparation strategies and potential interspecific competition among black-necked cranes, ruddy shelducks, and bar-headed geese prior to autumn migration, this study employed fecal DNA metabarcoding technology to conduct a high-resolution analysis of the food composition of these three bird species in Maduo County within the Sanjiangyuan National Park, enabling precise identification of food items at the species level. Regarding animal-based food, black-necked cranes exhibited strong specialization, showing a high preference for the tipulid species *T. subcunctans* (relative abundance 78.21%). Previous studies have shown that black-necked cranes consume *Tipula* insects before and after breeding(13); the larvae and pupae of Tipulidae also serve as important food for shorebirds and herons(14), and are rich in minerals such as phosphorus and magnesium that are crucial for avian health(15). This suggests that *T.* subcunctans plays a key role in the life history of black-necked cranes. In contrast, ruddy shelducks exhibited higher animal food diversity (Shannon index significantly higher than that of black-necked cranes, $P < 0.05$) and slightly higher, though not significantly, than that of bar-headed geese. Their main animal foods included: *M. orthocanna*, *Syllepte* sp., *K. bidentata*, *D. eugracilis*, *B. trispinosa*, *L. claparedianus*, and *C. circumdatus*. Bar-headed geese also consumed a relatively diverse range of animal foods, including *T. subcunctans*, *M. orthocanna*, *B. trispinosa*, *M. dasystomus*, *L. lunaris*, *E. guineensis*, *Euphyllia* sp., *C. bahamensis*, Cordyla sp., and *C. violaceus*. Thus, bar-headed geese share potential competition with black-necked cranes for animal food (e.g., *T. subcunctans*), and also share multiple common animal food items with ruddy shelducks. In terms of plant-based food, all three bird species commonly preferred *S. pectinata* (black-necked crane 22.31%, ruddy shelduck 63.55%, bar-headed goose 36.49%) and *C. hystericina* (black-necked crane 13.59%, ruddy shelduck 1.09%, bar-headed goose 16.47%). *S. pectinata* has abundant rhizomes and is a submerged plant with anti-inflammatory, antioxidant, and other medicinal properties(16–18). Although direct research on *C. hystericina* is limited, plants of the genus *Carex* are generally known to possess antibacterial, anti-inflammatory, anti-metabolic disease, and anti-tumor potential(19, 20). Additionally, black-necked cranes and bar-headed geese consumed large amounts of *A. anserina* (52.30% and 9.56%, respectively). This plant has enlarged tuberous roots(21) and is used as a tonic, food, and medicine in western China, exhibiting notable hepatoprotective and anti-inflammatory effects(22). Alpha diversity analysis further revealed dietary differentiation: for animal food, black-necked cranes had the lowest diversity, with the most specialized diet; ruddy shelducks had the highest diversity, preying on a wide range of available animals (insects, mollusks, etc.); bar-headed geese were intermediate, though differences with the other two groups were not statistically significant. For plant food, both black-necked cranes and ruddy shelducks concentrated on a few dominant plant species, but with distinct preferences and consumption abundances; bar-headed geese again occupied an intermediate position, consuming a

limited number of species but with relatively balanced proportions. Principal coordinate analysis (PCoA) showed that inter-group differences were greater than intra-group differences. LEfSe analysis further identified characteristic foods for each group: black-necked cranes were enriched for *T. subcunctans* and *A. anserina*; ruddy shelducks were enriched for *S. pectinata*, *R. carolinianus*, and various animals; bar-headed geese were enriched for *P. distans*, *C. hystericina*, and mosquitoes. These results clearly demonstrate trophic niche differentiation among the three bird species prior to autumn migration, which helps reduce interspecific food competition. This represents an important mechanism for sympatric species coexistence and a classic case of avoiding competition through niche differentiation in nature(23). Notably, the three medicinal plants *S. pectinata*, *C. hystericina*, and *A. anserina* together accounted for over 60% of the plant-based diet of the three bird species and should be key species of concern in conservation management efforts.

Analysis of the Gut Microbiota Composition of Three Bird Species and Its Adaptation to Diet

This study reports for the first time the gut microbiota composition of black-necked cranes, ruddy shelducks, and bar-headed geese just prior to autumn migration. At the phylum level, differences in microbiota composition profiles were observed among the three bird species. Black-necked cranes were dominated by Firmicutes_D (relative abundance 70.13%), followed by Actinobacteria, Proteobacteria, and Fusobacteria. Ruddy shelducks were also dominated by Firmicutes, with Firmicutes_D accounting for 25.23% and Firmicutes_A for 15.23%, followed by Actinobacteria, Proteobacteria, Bacteroidetes, and Chloroflexota. The major microbial composition of bar-headed geese was similar to that of ruddy shelducks, differing only in relative abundances. This result differs significantly from our previous observations made during the stable wintering period at Caohai Wetland in Guizhou (where Proteobacteria dominated(24)). Firmicutes and Proteobacteria play important roles in host digestion and metabolism(25–27), and the seasonal shift in microbiota composition may be closely related to the host's physiological state. LEfSe analysis revealed a close association between the enriched foods of the three bird species and their gut microbiota. The gut of black-necked cranes was significantly enriched with lactic acid bacteria, including *Ligilactobacillus* (45.15%) and *Carnobacterium* (12.54%). Lactic acid bacteria are beneficial microorganisms that stimulate digestive enzyme synthesis, improve feed utilization, and thereby promote host weight gain(28, 29), which is crucial for long-distance migration. Some lactic acid bacteria can ferment starch to produce short-chain fatty acids (SCFAs) while significantly increasing the relative abundances of beneficial genera such as *Ligilactobacillus* and *Roseburia*(30–32). SCFAs are not only important metabolic regulators(33, 34) but also play a key role in the high metabolic state of migratory birds(35). Furthermore, the main animal food of black-necked cranes, craneflies, contains chitin in their exoskeleton, which has been shown to promote the colonization of lactic acid bacteria in the gut of aquatic animals(36). This may similarly facilitate the proliferation of lactic acid bacteria in black-necked cranes, potentially contributing to their high proportion of Firmicutes. In autumn, ruddy shelducks primarily consumed a high-fiber plant-based diet consisting mainly of *S. pectinata* (63.55%) and *L. giganteum* (24.43%), while their animal food included

bivalves, various insects, and aquatic oligochaetes (all significantly enriched in their diet). A high-fiber diet requires the participation of cellulolytic/hemicellulolytic members of Firmicutes to ferment and produce SCFAs for energy. Like black-necked cranes, ruddy shelducks also harbored high proportions of *Lactobacillus* and *Carnobacterium* in their gut. In addition, they were significantly enriched in *Clostridium* (2.75%), a genus capable of utilizing various indigestible carbohydrates to ferment and produce SCFAs such as butyrate, acetate, and propionate, which are essential for maintaining intestinal barrier function, regulating immunity, and providing energy(37, 38). Bar-headed geese exhibited a diet intermediate between that of black-necked cranes and ruddy shelducks, with overlap with both species. Their gut microbial diversity was significantly higher than that of black-necked cranes and ruddy shelducks, and they harbored bacterial genera present in both of the other two species. Additionally, bar-headed geese were significantly enriched in *Enterococcus*, a genus identified by multiple studies as a key member of the lignocellulose-degrading microbial community (lignocellulose is the main component of plant cell walls(39, 40)), indicating that their gut microbiota is also adapted to a plant-based diet. Notably, the relative abundances of Proteobacteria in the autumn guts of all three bird species were low (black-necked crane 7.45%, ruddy shelduck 10.74%, bar-headed goose 13.33%), indicating that opportunistic pathogens were effectively suppressed under low-stress autumn conditions, and the gut remained in a stable state. In contrast, the cold winter environment and food scarcity alter intestinal motility, reduce blood flow, increase oxidative stress, and create conditions more favorable for Proteobacteria (which are generally more stress-tolerant) than for Firmicutes (which are more sensitive to pH and environmental changes(41)). Therefore, the high abundance of Firmicutes in autumn in these three bird species likely reflects a food-induced, anabolism-dominated energy storage strategy, whereas the high abundance of Proteobacteria in winter represents a stress-responsive survival strategy. Together, these patterns illustrate the complex role of gut microbiota as both a “sensor” and a “responder” of host physiological state(42, 43).

Integrated Analysis of Food, Microbiota, and Functional Pathways Reveals Metabolic Adaptation Strategies of Three Bird Species during the Autumn Migration Preparation Period

Black-necked cranes exhibit a typical "high metabolic activity state" during the autumn migration preparation period, characterized by a tight coupling among food composition, gut microbiota structure, and metabolic functional pathways. Spearman correlation analysis revealed that the plant foods *L. maritima* and *T. palustris* were positively correlated with multiple bacterial families. Among these, Marinilabiliaceae is a glycolytic bacterium capable of both respiratory and fermentative metabolism, degrading various sugars and proteins(44), and may participate in starch degradation(45), indicating that the gut microbiota of black-necked cranes broadly responds to their plant food. MetaCyc functional enrichment analysis showed that black-necked cranes co-enriched degradation pathways (carboxylic acid degradation, glycolysis, carbohydrate degradation) and biosynthesis pathways (cell structure biosynthesis, fatty acid and lipid biosynthesis, nucleoside and nucleotide biosynthesis), suggesting that they can efficiently break down carbon sources for energy while actively synthesizing fats and cellular structures. KEGG pathway analysis further confirmed significant enrichment in multiple pathways related to cell growth and death, nucleotide metabolism, membrane transport, glycan biosynthesis, translation,

and replication and repair, reflecting comprehensive high metabolic activity. Black-necked cranes typically migrate southward in October to the eastern Qinghai-Tibet Plateau or the Yunnan-Guizhou Plateau, adopting a rushed migration pattern of resting at night and flying continuously during the day(46, 47). Therefore, this high metabolic activity is inferred to represent substantial energy reserves in preparation for sustained flight, consistent with the previously described high proportion of *Ligilactobacillus* promoting short-chain fatty acid production, providing energy support and immune enhancement for intense migration. Notably, *C. maltaromaticum* (accounting for 8.25%) in the gut microbiota of black-necked cranes can also synthesize B vitamins such as pyridoxal, further optimizing host energy metabolism(9). In summary, the food, microbiota, and metabolic characteristics of black-necked cranes perfectly match the physiological demands of long-distance migration with efficient energy storage.

Ruddy shelducks exhibit a metabolic adaptation mode in autumn that prioritizes secondary metabolite synthesis. The association between their diet and microbiota is the most direct and significant: the high-fiber *S. pectinata* preferentially consumed by ruddy shelducks was positively correlated with cellulose-decomposing bacterial families: Cellulomonadaceae, Nocardioidaceae, and Eubacteriaceae. Cellulose-decomposing bacteria break down cellulose into glucose by secreting cellulase, providing energy for the host(13). Eubacteriaceae also participates in lignocellulose degradation; its genome carries multiple glycoside hydrolase genes that cleave xylan chains in plant cell walls and ferment carbohydrates to produce short-chain fatty acids(13, 48). In ruminant feces, this family may cooperate with other actinobacteria to degrade cellulose(49). KEGG analysis revealed significant enrichment in transcription and energy metabolism in ruddy shelducks, suggesting that they rely more on transcriptional regulation and energy production mechanisms to cope with diverse substrate inputs. MetaCyc functional enrichment analysis showed that ruddy shelducks were mainly enriched in biosynthesis pathways (aromatic compound biosynthesis, cell structure biosynthesis, fatty acid and lipid biosynthesis, amino acid biosynthesis), whereas degradation pathways were not significantly enriched. Spearman analysis indicated that amino acid metabolism was negatively correlated with *Chlorella* sp., *H. reticulatum*, and *Triceratium* sp.; glycolysis was positively correlated with *Chlorella* sp., *H. reticulatum*, and *Drosophila* sp., but negatively correlated with aquatic oligochaetes. These results indicate that ruddy shelducks focus more on the synthesis of secondary metabolites and structural components in autumn, which may be related to the need to synthesize various enzymes and metabolites to cope with diverse food sources(50).

Bar-headed geese exhibit the most unique metabolic adaptation mode, characterized by energy optimization rather than synthesis priority. In the bar-headed goose group, no significant correlations were found between any plant or animal food components and any gut microbial taxa. However, like black-necked cranes and ruddy shelducks, the gut microbiota of bar-headed geese established significant correlations with functional prediction pathways. KEGG analysis showed significant enrichment in transport and catabolism, signal transduction, cell motility, and biosynthesis of other secondary metabolites in bar-headed geese. From an evolutionary perspective, these pathway enrichments may reflect the deep adaptation of bar-headed geese to migratory life: transport and

catabolism ensure energy supply efficiency(51), signal transduction enhances environmental sensing and homeostasis regulation(52), cell motility optimizes muscle function and immune defense(53), and secondary metabolite biosynthesis provides a molecular basis for counteracting oxidative stress(54). Additionally, C1 compound utilization and assimilation, inorganic nutrient metabolism, electron transfer, nucleoside and nucleotide degradation, and cofactor and vitamin biosynthesis were significantly enriched in bar-headed geese, suggesting that they may generate C1 precursors such as formate through purine nucleotide degradation, which then enter folate-mediated one-carbon metabolism (C1 metabolism), providing an efficient conversion pathway for energy reserves before migration(55, 56). Notably, this metabolic state tends to maintain energy homeostasis rather than large-scale biosynthesis, forming a striking contrast with the traditional view that anabolism predominates before migration. Meanwhile, no significant difference in MetaCyc enrichment levels was found between the ruddy shelduck and bar-headed goose groups, indicating that their overall metabolic profiles are relatively similar, consistent with the cluster analysis results (the gut microbiota of bar-headed geese and ruddy shelducks are phylogenetically closer). Furthermore, across all three groups, all gut microbial taxa established significant positive or negative correlations with functional prediction pathways, whereas significant associations between food components and functional pathways occurred only in a few cases. This result strongly suggests that the impact of diet on gut microbiota function is much smaller than the impact of the gut microbiota itself on function.

The three sympatrically living bird species analyzed in this study exhibit significantly different metabolic strategies in facing autumn migration. This may be related to various factors including their migration route length, timing, diet, and physiological characteristics. Black-necked cranes have diverse migration routes: a comprehensive study based on satellite tracking data from 45 black-necked cranes revealed 11 different autumn migration routes(47). Juvenile cranes breeding in the Yanchiwan Nature Reserve in Gansu have an average migration distance of about 1,500 km, with prolonged stopovers at two long-term stopover sites, Da Qaidam and Chaka; black-necked cranes from Qinghai Lake and Jinzihu Wetland undertake long-distance (1455.7 ± 138.0 km) and prolonged (30.0 ± 10.6 d) autumn migrations(46). Most black-necked crane populations adopt a rushed mode of resting at night and flying continuously during the day(47), suggesting fundamental differences in migration urgency and energy management strategies among populations. Some studies indicate that migratory birds preferentially utilize omega-6 polyunsaturated fatty acids as fuel during long-distance flight, saving 11% of energy expenditure in the short term but possibly incurring a higher cost of oxidative damage over the long term(57). The pattern of consuming short-chain fatty acids adopted by black-necked cranes in this study may force them to adopt a rushed migration rhythm to avoid the accumulation of oxidative damage. Ruddy shelducks can fly over the Himalayas from wintering grounds in India and Bangladesh to breeding grounds such as Qinghai Lake in China, Mongolia, and Russia, establishing a direct connection between the Indian subcontinent wintering grounds and the Qinghai-Tibet Plateau breeding grounds(58, 59), demonstrating their remarkable physiological adaptability. In the Qinghai Lake region, ruddy shelducks rely primarily on plant food as an energy source, with a relatively low trophic level(60), indicating that their energy accumulation before autumn migration depends mainly on plant resources, consistent with the finding in

this study that ruddy shelducks obtain energy through cellulose degradation. The year-round range of bar-headed geese is mainly confined to the interior of the Qinghai-Tibet Plateau (e.g., populations from Qinghai Lake to Shigatse Prefecture in Tibet(61)). Similar to bar-headed geese, the white stork (Ciconia ciconia) has adopted an energy-saving migration strategy, significantly improving juvenile survival in recent years by "wintering nearby," demonstrating the direct survival benefits of energy-saving behavior. Previous studies have confirmed that during hypoxic flight, bar-headed geese do not simply increase heart rate to enhance oxygen supply but instead actively reduce metabolic rate to match limited oxygen availability(62, 63), which is highly consistent with the results of this study. The above data and discussion are mainly based on research findings from the Qinghai Lake region. Specific migration routes of black-necked cranes, ruddy shelducks, and bar-headed geese within the Sanjiangyuan National Park have not yet been reported. Given that the two regions are approximately 150 km apart, it is speculated that their migration patterns may be similar to the data from Qinghai Lake. Future research should integrate the specific migration routes of the three bird species within Sanjiangyuan Park with metagenomics and metabolomics for further validation.

Conclusions

This study, utilizing mitochondrial *COI* and chloroplast *rbcL* gene sequencing alongside *16S rRNA* amplicon sequencing, combined with Spearman correlation analysis and metabolic pathway enrichment (MetaCyc/KEGG) analysis, for the first time systematically reveals the differences in diet composition, gut microbiota structure, and metabolic functions of sympatrically distributed black-necked cranes, ruddy shelducks, and bar-headed geese in the Sanjiangyuan National Park during the autumn migration preparation period. It elucidates the differentiated adaptive strategies employed by these three bird species in response to the energy demands of migration. The main conclusions are as follows: (1) The three bird species exhibit significant trophic niche differentiation prior to autumn migration. Black-necked cranes are highly enriched for the *T. subcunctans* and *A. anserina*; ruddy shelducks are enriched for *S. pectinata*, *R. carolinianus*, and various animals; bar-headed geese are enriched for *P. distans* and *C. hystericina*. This niche differentiation represents an important mechanism enabling their sympatric coexistence. Notably, three medicinal plants, *S. pectinata*, *C. hystericina*, and *A. anserina* together account for over 60% of the plant-based diet of the three bird species and should be prioritized as key species for conservation and management. (2) Black-necked cranes primarily feed on high-starch tuberous roots (*A. anserina*) and chitin-rich *T. subcunctans*. Chitin promotes the colonization of gut lactic acid bacteria (*Ligilactobacillus* 45.15%, *Carnobacterium* 12.54%), which can stimulate digestive enzyme synthesis, improve feed utilization, and thereby promote weight gain. Functionally, black-necked cranes simultaneously enhance catabolism and anabolism, displaying a typical "high metabolic activity state." This strategy enables them to rapidly convert high-starch food into fat reserves to meet the energy demands of migration. (3) Ruddy shelducks feed on high-fiber *S. pectinata* and a variety of animals. Their gut Firmicutes composition is diverse, including cellulose-decomposing bacteria such as Cellulomonadaceae and Eubacteriaceae, as well as genera including *Clostridium*, *Romboutsia*, and *Streptococcus*. Cellulomonadaceae and Eubacteriaceae are responsible for breaking down cellulose into

short-chain fatty acids, providing energy for the host. Functionally, ruddy shelducks are mainly enriched in anabolic pathways and finely regulate metabolic output through transcriptional control. This strategy allows them to flexibly cope with diverse food sources, achieving a balance between energy acquisition and anabolism. (4) Bar-headed geese consume a variety of plants (including *S. pectinata*, *P. distans*, *Carex* sp., and *A. anserina*) as well as animals, but no significant correlation was found between their dietary components and gut microbiota. Functionally, bar-headed geese are significantly enriched in pathways related to C1 compound utilization, electron transfer, and nucleotide degradation, with a dominance of energy optimization and catabolism, tending to maintain energy homeostasis rather than large-scale biosynthesis. This strategy may reflect their "energy-saving" adaptation for long-distance migration, consistent with previous findings that bar-headed geese actively reduce their metabolic rate during hypoxic flight.

The differentiated strategies of the three bird species reveal lineage-specific adaptations in energy management among high-altitude migratory species: black-necked cranes rely on microbiota-mediated energy storage enhancement to cope with peak energy demands during migration; ruddy shelducks depend on microbiota plasticity to achieve dietary generalization; bar-headed geese optimize basal metabolism for energy conservation through functional stability of the gut microbiota. This study finds that the contribution of the gut microbiota itself to function is much greater than the direct contribution of dietary components, suggesting that research on host- microbe interactions should pay more attention to the intrinsic metabolic potential of the microbiota rather than focusing solely on dietary inputs. These results not only provide new scientific insights into the microbial mechanisms underlying the migratory energetics of birds but also establish a theoretical foundation for the management of food resources in wetland conservation. Future research should integrate multi-omics approaches to further dissect the molecular mechanisms of host, microbiota and environment interactions, particularly the regulatory relationship between short-chain fatty acid signaling pathways and host energy allocation decisions.

Declarations

Abbreviations

Not applicable

Ethics approval and consent to participate

This research was approved by the Research Ethics Committee of Guizhou Normal University (Approval No. 2026030019). During the fieldwork, we only collected feces from the foraging grounds of Black-necked Cranes, Ruddy Shelducks, and Bar-headed Geese; no capture or any direct manipulation or disturbance of these birds was involved. The fecal sample collection strictly complied with the Wildlife Protection Law of the People's Republic of China and the local administrative regulations of Sanjiangyuan National Park.

Consent for publication

Not applicable

Competing Interests

The authors declare that they have no conflicts of interest.

Funding

This study was supported by the following funds: the Joint Grant from Chinese Academy of Sciences-People's Government of Qinghai Province on Sanjiangyuan National Park (LHZX-2023-02); the 2023 Award Fund of the Qinghai Provincial Key Laboratory of Animal Ecological Genomics (Grant No. QHEG-2025-04); the Cultivation Project of the National Natural Science Foundation of China at Guizhou Normal University (Grant/Award No. Guojia Peiyu [2026] No. 13); and the 2026 Independent Cultivation Project for Quality Improvement and Expansion - Biology Group (Grant No. 209- C426002).

Author Contribution

Y-YW designed the experiments, analyzed the data, and wrote the original draft. MF and AW performed the DNA extraction and PCR amplification. FJ collected fecal samples from black-necked cranes, ruddy shelducks, and bar-headed geese, and reviewed and edited the manuscript.

Acknowledgement

We thank the Sanjiangyuan National Park for assistance with sample collection.

Data Availability

The original sequences of Black-necked Cranes, Ruddy Shelducks and Bar-headed Geese have been deposited in GenBank under accession numbers: PRJNA1463505.

References

1. Wambugu GM, Amakobe B, Şekercioğlu ÇH, Githiru M. Elevational patterns of species richness and community structure of understorey birds in an East African montane forest. Afr J Ecol. 2024;62(1):e13235. 10.1111/aje.13235.
2. Scridel D, Anderle M, Capelli F, Forti A, Bettega C, Alessandrini C, et al. Coping with unpredictable environments: fine-tune foraging microhabitat use in relation to prey availability in an alpine species.

Oecologia. 2024;204(4):845–60. 10.1007/s00442-024-05530-1.

3. Zhao X, Che X, Ning T, Zou F. Distribution of birds in the high-altitude area of Mount Everest. Integr Zool. 2023;18(1):199–204. 10.1111/1749-4877.12617.
4. Ribeiro ÂM, Puetz L, Pattinson NB, Dalén L, Deng Y, Zhang G, et al. 31° South: The physiology of adaptation to arid conditions in a passerine bird. Mol Ecol. 2019;28(16):3709–21. 10.1111/mec.15176.
5. Muegge BD, Kuczynski J, Knights D, Clemente JC, González A, Fontana L, et al. Diet Drives Convergence in Gut Microbiome Functions Across Mammalian Phylogeny and Within Humans. Science. 2011;332(6032):970–4. 10.1126/science.1198719.
6. Kohl KD, Brun A, Magallanes M, Brinkerhoff J, Laspiur A, Acosta JC, et al. Gut microbial ecology of lizards: insights into diversity in the wild, effects of captivity, variation across gut regions and transmission. Mol Ecol. 2017;26(4):1175–89. 10.1111/mec.13921.
7. Fu H, Zhang L, Fan C, Li W, Liu C, Zhang H, et al. Sympatric Yaks and Plateau Pikas Promote Microbial Diversity and Similarity by the Mutual Utilization of Gut Microbiota. Microorganisms. 2021;9(9):1890. 10.3390/microorganisms9091890.
8. Lu Z, Li S, Wang M, Wang C, Meng D, Liu J. Comparative Analysis of the Gut Microbiota of Three Sympatric Terrestrial Wild Bird Species Overwintering in Farmland Habitats. Front Microbiol. 2022;13:905668. 10.3389/fmicb.2022.905668.
9. Li W, Zhao J, Tian H, Shen Y, Wang Y, Shao M, et al. Gut microbiota enhance energy accumulation of black-necked crane to cope with impending migration. Appl Microbiol Biotechnol. 2023;107(14):4635–46. 10.1007/s00253-023-12598-x.
10. Li W, Cheng L, He X, He G, Liu Y, Sang Z, et al. Gut fungi of black-necked cranes (Grus nigricollis) respond to dietary changes during wintering. BMC Microbiol. 2024;24(1):232. 10.1186/s12866-024-03396-0.
11. Zhang Y, Ma R, Suolangduoerji, Ma S, Nuertai A, He K, et al. Annual cycle variations in the gut microbiota of migratory black-necked cranes. Front Microbiol. 2025;16:1533282. 10.3389/fmicb.2025.1533282.
12. Zhang S, Zhou C, Dong Z, Feng K, Peng K, Wang Z, et al. The diet–intestinal microbiota dynamics and adaptation in an elevational migration bird, the Himalayan bluetail (*Tarsiger rufilatus*). Ecol Evol. 2024;14(7):e11617. 10.1002/ece3.11617.
13. Ma R, Ma S, Liu H, Hu L, Li Y, He K, et al. Seasonal changes in invertebrate diet of breeding black-necked cranes (*Grus nigricollis*). Ecol Evol. 2024;14(9):e70234. 10.1002/ece3.70234.
14. Brugman V. Host selection and feeding preferences of farm-associated mosquitoes (Diptera: Culicidae) in the United Kingdom [Internet]. 2016. 10.17037/PUBS.02548573
15. Yin W, Liu J, Liu H, Lv B, Nutritional Value. Food Ingredients, Chemical and Species Composition of Edible Insects in China. In: Mikkola H, editor. Future Foods [Internet]. InTech; 2017 [cited 2026 May 19]. Available from: http://www.intechopen.com/books/future-foods/nutritional-value-food-

ingredients-chemical-and-species-composition-of-edible-insects-in-china 10.5772/intechopen.70085

16. Anna MK, Vimala KS, Raiby P, Paul, Priyalatha B, Priya S. Phytoremediation potential of a few hydrophytic medicinal plants: A review. Int J Sch Res Biol Pharm. 2023;2(1):005–9. 10.56781/ijsrbp.2023.2.1.0013.
17. Waridel P. Investigation phytochimique des plantes aquatiques Potamogeton pectinatus L., P. lucens L., P. perfoliatus L. et P. crispus L. (Potamogetonaceae) [Thesis]. [Lausanne, Switzerland]: Université de Lausanne; 2003.
18. Ghobrial MG. Recent vegetations biodiversity in Nile Delta wetlands in Egypt. In. Journal of Biodiversity & Endangered Species; 2021. Available from: https://www.scitechnol.com/proceedings/recent-vegetations-biodiversity-in-nile-delta-wetlands-in-egypt-92.html
19. Du P, Liu B, Wang X, Zheng Z, Liu S, Guan S, et al. Carex meyeriana Kunth Extract Is a Novel Natural Drug against Candida albicans. Int J Mol Sci. 2024;25(13):7288. 10.3390/ijms25137288.
20. Dávid CZ, Kúsz N, Agbadua OG, Berkecz R, Kincses A, Spengler G, et al. Phytochemical Investigation of Carex praecox Schreb. and ACE-Inhibitory Activity of Oligomer Stilbenes of the Plant. Molecules. 2024;29(14):3427. 10.3390/molecules29143427.
21. Huang Y, Yang J, Zhao G, Yang Y. Potential Distribution and Cultivation Areas of Argentina anserina (Rosaceae) in the Upper Reaches of the Dadu River and Minjiang River Basin Under Climate Change: Applications of Ensemble and Productivity Dynamic Models. Biology. 2025;14(6):668. 10.3390/biology14060668.
22. Yang D, Han N, Wang YW, Zhai JX, Liu ZH, Li SK, et al. Pentacyclic Triterpenoid Saponins, Poterinasides A–J, from Silverweed Cinquefoil Roots Promising Hepatoprotective and Anti-inflammatory Agents. J Org Chem. 2021;86(16):11220–36. 10.1021/acs.joc.1c00812.
23. Guibert I, Conti-Jerpe IE, Pons L, Tayaban K, Sayco SL, Cabaitan P et al. Trophic niche partitioning in symbiotic marine invertebrates [Internet]. Ecology; 2024 [cited 2026 May 19]. Available from: http://biorxiv.org/lookup/doi/10.1101/2024.02.05.578332 doi:10.1101/2024.02.05.578332.
24. Wang F, Yang Y, Song G, Shi X, Pu B, Yang L. Mangcuo Lake in Hengduan Mountains: An Important Alpine Breeding and Stopover Site along Central Asian Flyway. Animals. 2023;13(7):1139. 10.3390/ani13071139.
25. Kaoutari AE, Armougom F, Gordon JI, Raoult D, Henrissat B. The abundance and variety of carbohydrate-active enzymes in the human gut microbiota. Nat Rev Microbiol. 2013;11(7):497–504. 10.1038/nrmicro3050.
26. Shin NR, Whon TW, Bae JW. Proteobacteria: microbial signature of dysbiosis in gut microbiota. Trends Biotechnol. 2015;33(9):496–503. 10.1016/j.tibtech.2015.06.011.
27. Yang SH, Ahn HK, Kim BS, Chang SS, Chung KY, Lee EM, et al. Comparison of bacterial communities in leachate from decomposing bovine carcasses. Asian-Australas J Anim Sci. 2017;30(11):1660–6. 10.5713/ajas.17.0553.

28. Xu Y, Chen K, Huang Y, Yan Y, Zhang W, Tian J, et al. Fecal microbiota transplantation improves growth performance of chickens by increasing the intestinal Lactobacillus and glutamine. Poult Sci. 2025;104(8):105243. 10.1016/j.psj.2025.105243.
29. Yang J, Wang J, Liu Z, Chen J, Jiang J, Zhao M, et al. Ligilactobacillus Salivarius improve body growth and anti-oxidation capacity of broiler chickens via regulation of the microbiota-gut-brain axis. BMC Microbiol. 2023;23(1):395. 10.1186/s12866-023-03135-x.
30. Sun H, Du Z, Fan L, Xu Z, Yang W, Zhang G, et al. Structural alterations in butyrylated and recrystallized high-amylose maize starch and their effect on gut microbiota during in vitro fermentation. Int J Biol Macromol. 2025;302:139970. 10.1016/j.ijbiomac.2025.139970.
31. Shao D, Zhang J, Shao T, Li Y, He H, Wang Y, et al. Modification of Structure, Pasting, and In Vitro Digestion Properties of Glutinous Rice Starch by Different Lactic Acid Bacteria Fermentation. Foods. 2025;14(3):367. 10.3390/foods14030367.
32. Cele NP, Kewuyemi YO, Adiamo O, Bobasa EM, Zhang J, Seididamyeh M, et al. Probiotic Lactic Acid Bacteria-Fermented Beverages from Bambara Groundnut and Cowpea Sprouts Modulate Gut Microbiota and Short-Chain Fatty Acids. Foods. 2026;15(7):1141. 10.3390/foods15071141.
33. Rauf A, Khalil AA, Rahman U ur, Khalid A, Naz S, Shariati MA et al. Recent advances in the therapeutic application of short-chain fatty acids (SCFAs): An updated review. Crit Rev Food Sci Nutr. 2022;62(22):6034–54. 10.1080/10408398.2021.1895064
34. Mukhopadhya I, Louis P. Gut microbiota-derived short-chain fatty acids and their role in human health and disease. Nat Rev Microbiol. 2025;23(10):635–51. 10.1038/s41579-025-01183-w.
35. Gupta NJ, Das S, Das M, Arya R, Kumar A, Nanda RK. Seasonal plasticity and energy efficiency in migratory buntings is an assemblage of alterations in metabolic and gut microbe adaptations [Internet]. Animal Behavior and Cognition; 2023 [cited 2026 May 19]. Available from: http://biorxiv.org/lookup/doi/10.1101/2023.02.17.529037 doi:10.1101/2023.02.17.529037.
36. Leeper A, Benhaïm D, Smárason BÖ, Knobloch S, Òmarsson KL, Bonnafoux T, et al. Feeding black soldier fly larvae (Hermetia illucens) reared on organic rest streams alters gut characteristics of Atlantic salmon (Salmo salar). J Insects Food Feed. 2022;8(11):1355–72. 10.3920/JIFF2021.0105.
37. Corte V, Andrade AC, Diaz-Bulnes P, Salazar Garzo N, Bande JJ, Sanchez-Alvarez JE, MO046MICROBIOTA DERIVED SHORT CHAIN FATTY ACIDS, PROPIONATE AND BUTYRATE, CONTRIBUTE TO MODULATE THE INFLAMMATORY RESPONSE IN CHRONIC KIDNEY DISEASE, et al. Nephrol Dial Transpl. 2020;35(Supplement3):gfaa140MO046. 10.1093/ndt/gfaa140.MO046.
38. Fu X, Liu Z, Zhu C, Mou H, Kong Q. Nondigestible carbohydrates, butyrate, and butyrate-producing bacteria. Crit Rev Food Sci Nutr. 2019;59(sup1):S130–52. 10.1080/10408398.2018.1542587.
39. Zhu J, Liu J, Li W, Ru Y, Sun D, Liu C, et al. Dynamic changes in community structure and degradation performance of a bacterial consortium MMBC-1 during the subculturing revival reveal the potential decomposers of lignocellulose. Bioresour Bioprocess. 2022;9(1):110. 10.1186/s40643-022-00601-8.

40. Gan Y, Wu Y, jun, Dong Y, qiu, Li Q, Wu Sguang, Jin Y et al. qing,. The study on the impact of sex on the structure of gut microbiota of bamboo rats in China. Front Microbiol. 2023;14:1276620. 10.3389/fmicb.2023.1276620
41. Ichikawa N, Sasaki H, Lyu Y, Furuhashi S, Watabe A, Imamura M, et al. Cold Exposure during the Active Phase Affects the Short-Chain Fatty Acid Production of Mice in a Time-Specific Manner. Metabolites. 2021;12(1):20. 10.3390/metabo12010020.
42. Jones RM, Neish AS. Redox signaling mediated by the gut microbiota. Free Radic Biol Med. 2017;105:41–7. 10.1016/j.freeradbiomed.2016.10.495.
43. Wojciech L, Png CW, Koh EY, Kioh DYQ, Deng L, Wang Z, et al. A tryptophan metabolite made by a gut microbiome eukaryote induces pro-inflammatory T cells. EMBO J. 2023;42(21):e112963. 10.15252/embj.2022112963.
44. Suzuki M et al. *Marinilabilia*. In: Trujillo ME, Dedysh S, DeVos P, Hedlund B, Kämpfer P, Rainey FA, editors. Bergey's Manual of Systematics of Archaea and Bacteria [Internet]. 1st ed. Wiley; 2015 [cited 2026 May 19]. pp. 1–4. Available from: https://onlinelibrary.wiley.com/doi/10.1002/9781118960608.gbm00241 doi:10.1002/9781118960608.gbm00241.
45. Zeng Y, Qiu Y, Wang Y, Zhang X, Wang D, Chen X, et al. Effects of γ-ray irradiation on insect pests, physicochemical properties, and microbial community of strong-flavor Daqu during maturation. Appl Radiat Isot. 2025;220:111780. 10.1016/j.apradiso.2025.111780.
46. Wang W, Wang F, Li L, Wang A, Sharshov K, Druzyaka A, et al. Characterization of the gut microbiome of black-necked cranes (Grus nigricollis) in six wintering areas in China. Arch Microbiol. 2020;202(5):983–93. 10.1007/s00203-019-01802-0.
47. Pu Z, Guo Y. Autumn migration of black-necked crane (*Grus nigricollis*) on the Qinghai-Tibetan and Yunnan-Guizhou plateaus. Ecol Evol. 2023;13(9):e10492. 10.1002/ece3.10492.
48. Zhang Y, Tan H, Deng Q, Cao L. Actinobacterial Flora in Feces of Healthy Cottontail Rabbits (Sylvilagus auduboni). Probiotics Antimicrob Proteins. 2015;7(1):9–13. 10.1007/s12602-014-9179-x.
49. Tan H, Deng Q, Cao L. Ruminant feces harbor diverse uncultured symbiotic actinobacteria. World J Microbiol Biotechnol. 2014;30(3):1093–100. 10.1007/s11274-013-1529-4.
50. Wang W, Zheng S, Li L, Yang Y, Liu Y, Wang A, et al. Comparative metagenomics of the gut microbiota in wild greylag geese (*Anser anser*) and ruddy shelducks (*Tadorna ferruginea*). MicrobiologyOpen. 2019;8(5):e00725. 10.1002/mbo3.725.
51. Dong H, Zhang J, Li Y, Ahmad HI, Li T, Liang Q, et al. Liver Transcriptome Profiling Identifies Key Genes Related to Lipid Metabolism in Yili Geese. Animals. 2023;13(22):3473. 10.3390/ani13223473.
52. Kanehisa M, Furumichi M, Sato Y, Matsuura Y, Ishiguro-Watanabe M. KEGG: biological systems database as a model of the real world. Nucleic Acids Res. 2025;53(D1):D672–7. 10.1093/nar/gkae909.

53. Yoodee S, Peerapen P, Plumworasawat S, Malaitad T, Thongboonkerd V. Identification and characterization of ARID1A-interacting proteins in renal tubular cells and their molecular regulation of angiogenesis. J Transl Med. 2023;21(1):862. 10.1186/s12967-023-04750-y.
54. Huckvale ED, Moseley HNB. Predicting the Pathway Involvement of All Pathway and Associated Compound Entries Defined in the Kyoto Encyclopedia of Genes and Genomes. Metabolites. 2024;14(11):582. 10.3390/metabo14110582.
55. García JL, Galán B. Integrating greenhouse gas capture and C1 biotechnology: a key challenge for circular economy. Microb Biotechnol. 2022;15(1):228–39. 10.1111/1751-7915.13991.
56. Hankofer V, Ghirardo A, Obermaier L, Poschet G, Kumar JS, Gross I, et al. Photorespiration is linked to DNA methylation by formate as a one-carbon source. Nat Plants. 2026;12(3):653–64. 10.1038/s41477-026-02222-x.
57. McWilliams S, Pierce B, Wittenzellner A, Langlois L, Engel S, Speakman JR, et al. The energy savings-oxidative cost trade-off for migratory birds during endurance flight. eLife. 2020;9:e60626. 10.7554/eLife.60626.
58. Gilbert M, Newman SH, Takekawa JY, Loth L, Biradar C, Prosser DJ, et al. Flying Over an Infected Landscape: Distribution of Highly Pathogenic Avian Influenza H5N1 Risk in South Asia and Satellite Tracking of Wild Waterfowl. EcoHealth. 2010;7(4):448–58. 10.1007/s10393-010-0672-8.
59. Li D, Davison G, Lisovski S, Battley PF, Ma Z, Yang S, et al. Shorebirds wintering in Southeast Asia demonstrate trans-Himalayan flights. Sci Rep. 2020;10(1):21232. 10.1038/s41598-020-77897-z.
60. Yang Yqin, Yi X, feng, Li N. Analysis on Trophic Structure of Main Waterbirds in Qinghai Lake Based on Stable Isotopic Technology: Analysis on Trophic Structure of Main Waterbirds in Qinghai Lake Based on Stable Isotopic Technology. Zool Res. 2009;30(4):418–22. 10.3724/SP.J.1141.2009.04418.
61. Zhang J, Deng X, Xie Y, Li L, Batbayar N, Damba I, et al. The importance of the Qinghai-Tibet Plateau for Bar-headed Geese Anser indicus: results from GPS/GSM telemetry. Wildfowl. 2020;70:57–75.
62. Meir JU, York JM, Chua BA, Jardine W, Hawkes LA, Milsom WK. Reduced metabolism supports hypoxic flight in the high-flying bar-headed goose (Anser indicus). eLife. 2019;8:e44986. 10.7554. /eLife.44986 PubMed PMID: 31478481; PubMed Central PMCID: PMC6721836.
63. Harrison J. The highs and lows of bird flight. eLife. 2019;8:e50626. 10.7554. /eLife.50626 PubMed PMID: 31478484; PubMed Central PMCID: PMC6721789.
64. Leray M, Yang JY, Meyer CP, Mills SC, Agudelo N, Ranwez V, et al. A new versatile primer set targeting a short fragment of the mitochondrial COI region for metabarcoding metazoan diversity: application for characterizing coral reef fish gut contents. Front Zool. 2013;10(1):34. 10.1186/1742-9994-10-34.
65. Yu DW, Ji Y, Emerson BC, Wang X, Ye C, Yang C, et al. Biodiversity soup: metabarcoding of arthropods for rapid biodiversity assessment and biomonitoring. Methods Ecol Evol. 2012;3(4):613–23. 10.1111/j.2041-210X.2012.00198.x.

66. Hofreiter M, Poinar HN, Spaulding WG, Bauer K, Martin PS, Possnert G, et al. A molecular analysis of ground sloth diet through the last glaciation. Mol Ecol. 2000;9(12):1975–84. 10.1046/j.1365-294X.2000.01106.x.
67. Poinar HN, Hofreiter M, Spaulding WG, Martin PS, Stankiewicz BA, Bland H, et al. Molecular Coproscopy: Dung and Diet of the Extinct Ground Sloth *Nothrotheriops shastensis*. Science. 1998;281(5375):402–6. 10.1126/science.281.5375.402.
68. Mori H, Maruyama F, Kato H, Toyoda A, Dozono A, Ohtsubo Y, et al. Design and Experimental Application of a Novel Non-Degenerate Universal Primer Set that Amplifies Prokaryotic 16S rRNA Genes with a Low Possibility to Amplify Eukaryotic rRNA Genes. DNA Res. 2014;21(2):217–27. 10.1093/dnares/dst052.
69. Bolyen E, Rideout JR, Dillon MR, Bokulich NA, Abnet CC, Al-Ghalith GA, et al. Reproducible, interactive, scalable and extensible microbiome data science using QIIME 2. Nat Biotechnol. 2019;37(8):852–7. 10.1038/s41587-019-0209-9.
70. Callahan BJ, McMurdie PJ, Rosen MJ, Han AW, Johnson AJA, Holmes SP. DADA2: High-resolution sample inference from Illumina amplicon data. Nat Methods. 2016;13(7):581–3. 10.1038/nmeth.3869.
71. DeSantis TZ, Hugenholtz P, Larsen N, Rojas M, Brodie EL, Keller K, et al. Greengenes, a Chimera-Checked 16S rRNA Gene Database and Workbench Compatible with ARB. Appl Environ Microbiol. 2006;72(7):5069–72. 10.1128/AEM.03006-05.
72. Rognes T, Flouri T, Nichols B, Quince C, Mahé F. VSEARCH: a versatile open source tool for metagenomics. PeerJ. 2016;4:e2584. 10.7717/peerj.2584.
73. Nilsson RH, Ryberg M, Kristiansson E, Abarenkov K, Larsson KH, Kõljalg U. Taxonomic Reliability of DNA Sequences in Public Sequence Databases: A Fungal Perspective. Fairhead C, editor. PLoS ONE. 2006;1(1):e59. 10.1371/journal.pone.0000059
74. Oksanen J, Blanchet FG, Kindt R, Legendre P, O'hara RB, Simpson GL et al. The vegan Package. Community Ecology Package [Internet]. 2010. Available from: https://cran.r-project.org/src/contrib/Archive/vegan/
75. Langille MGI, Zaneveld J, Caporaso JG, McDonald D, Knights D, Reyes JA, et al. Predictive functional profiling of microbial communities using 16S rRNA marker gene sequences. Nat Biotechnol. 2013;31(9):814–21. 10.1038/nbt.2676.

Figures

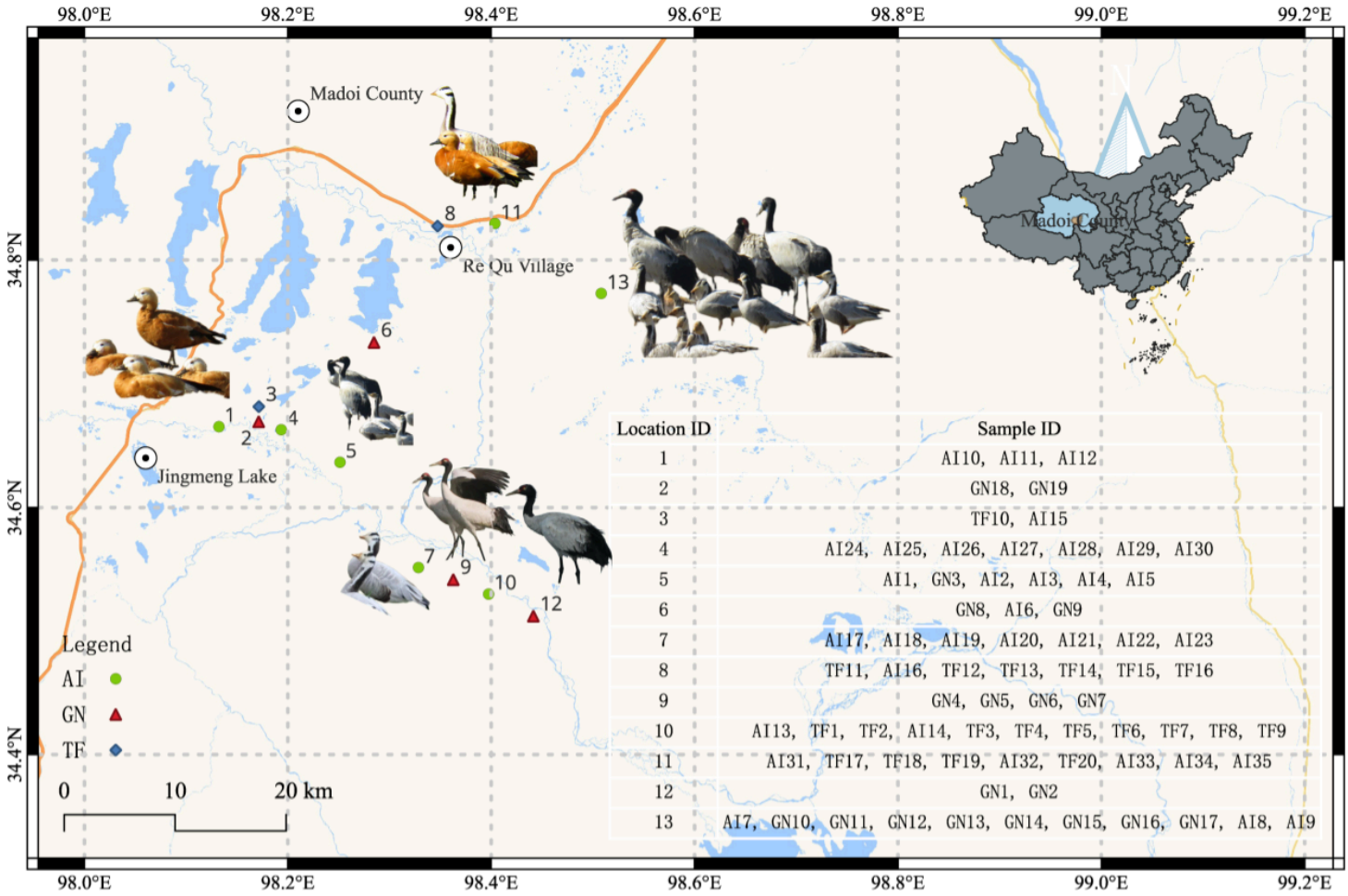

Figure 1

Fecal sampling sites of *G. nigricollis* (GN), *T. ferruginea* (TF), and *A. indicus* (AI) in Madoi County, Sanjiangyuan National Park, Qinghai Province, China.

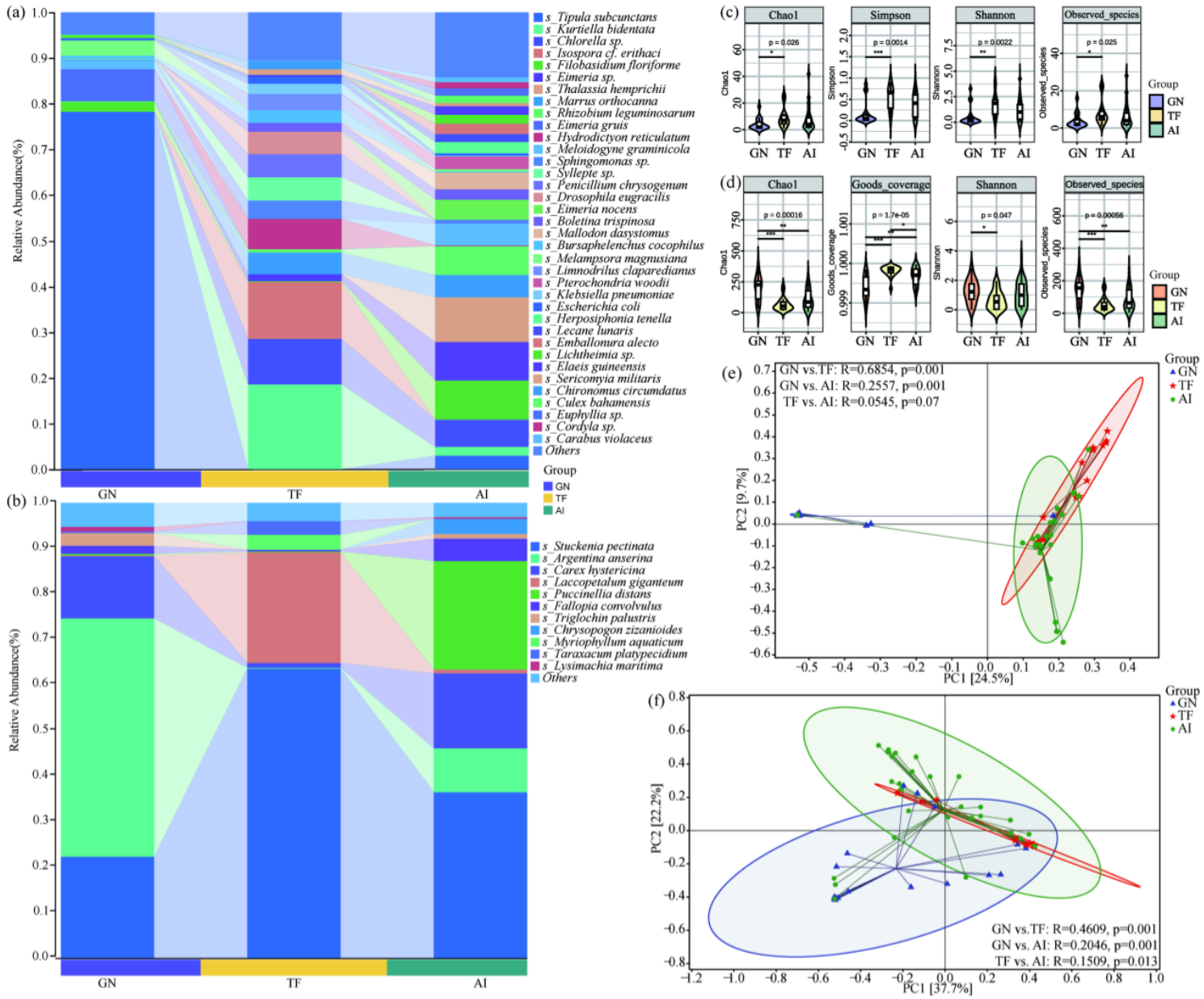

Figure 2

Species composition (relative abundance >1%) by *COI* sequencing (a); herbivorous diet composition (>1%) by *rbcL* sequencing (b); significant alpha diversity indices from *COI* (c); significant alpha diversity indices from *rbcL* (d); PCoA of *COI* results (e); PCoA of *rbcL* results (f).

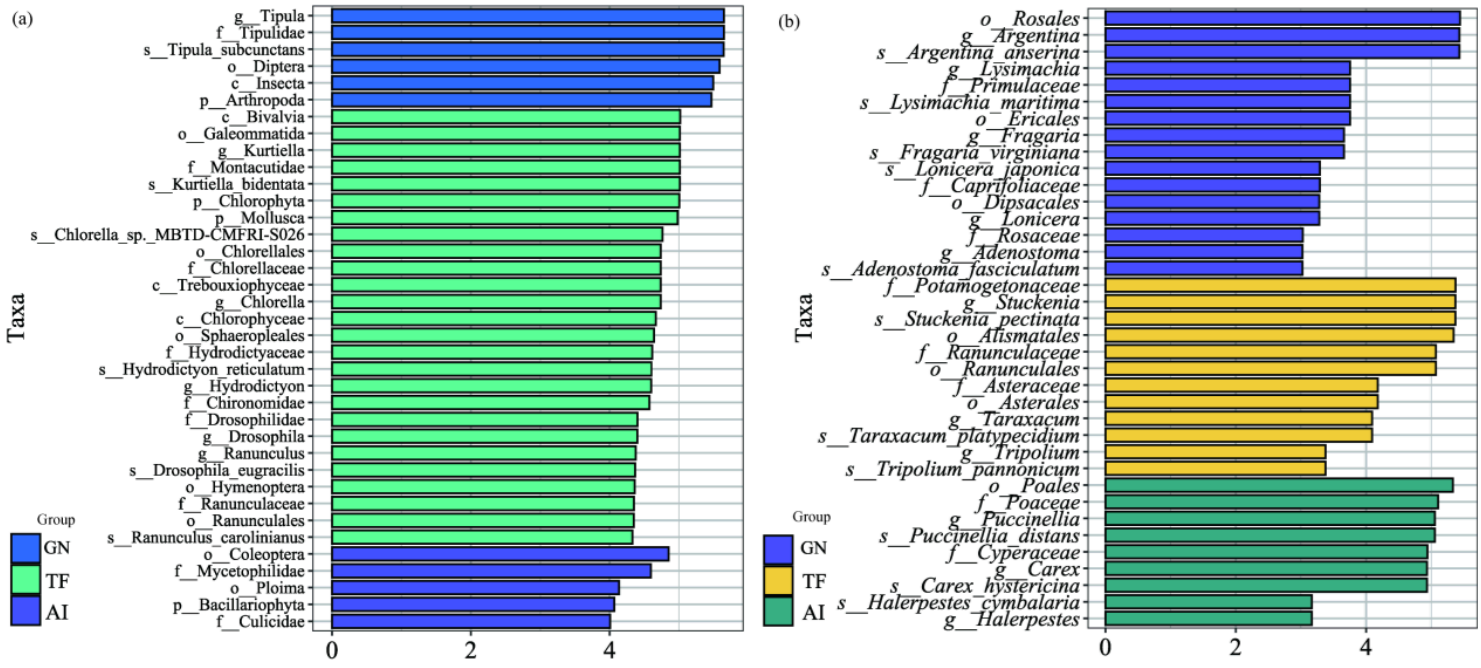

Figure 3

LEfSe analysis of animal-based (a) and plant-based (b) food composition of *G. nigricollis* (GN), *T. ferruginea* (TF), and *A. indicus* (AI).

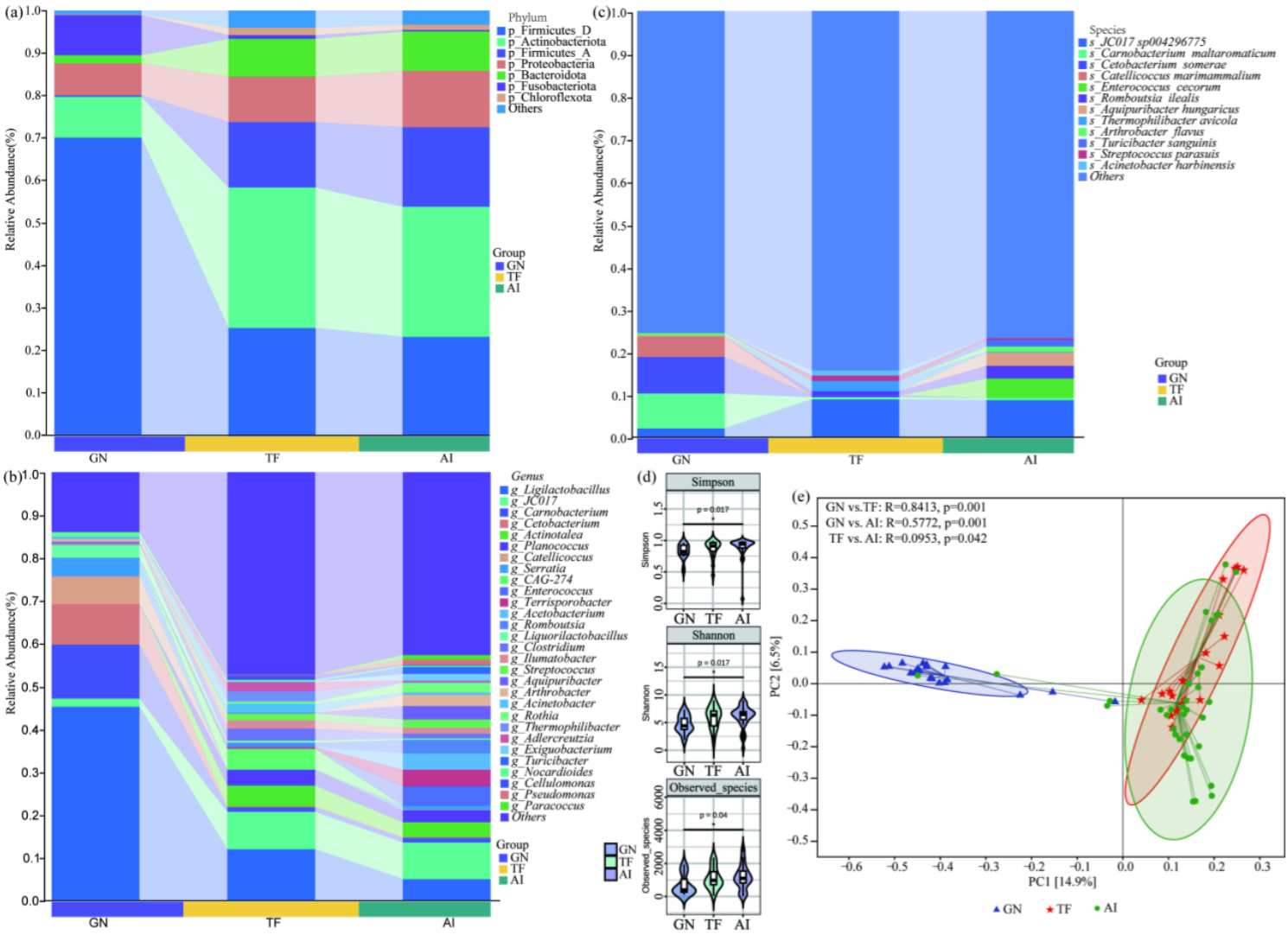

Figure 4

Composition of gut microbiota at the phylum (a), genus (b), and species (c) levels. Significantly different alpha diversity (d) and PCoA analysis (e) of gut microbiota.

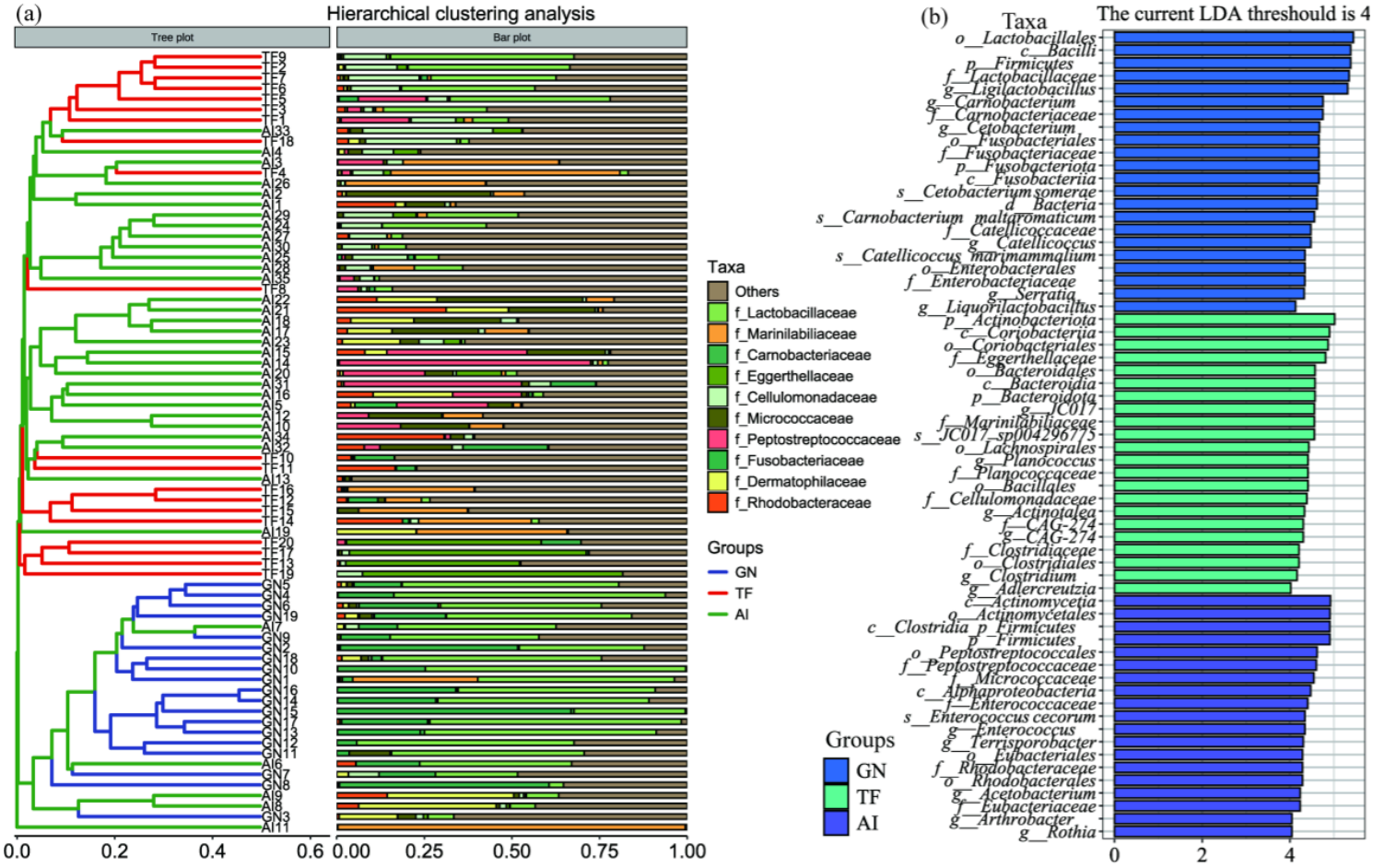

Figure 5

Cluster analysis (a) and LEfSe analysis (b) of gut microbiota in *G. nigricollis* (GN), *T. ferruginea* (TF), and *A. indicus*(AI).

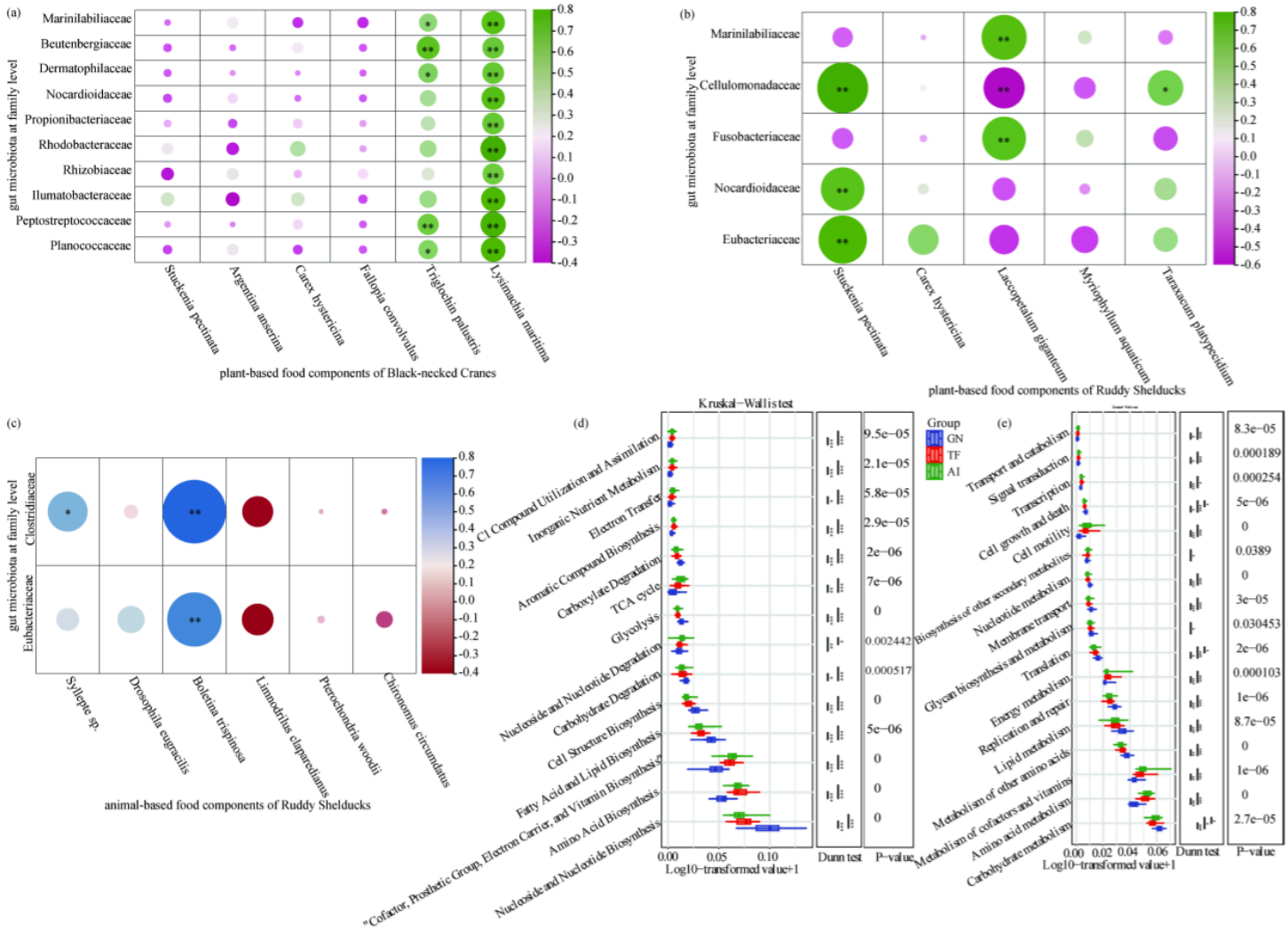

Figure 6

Correlations between gut microbiota and plant-based food components of *G. nigricollis* (a) and *T. ferruginea*(b) by Spearman. Correlations between gut microbiota and animal-based food components of *T. ferruginea* (c) by Spearman. Significant differences in metabolic function relative abundance among GN, TF, and AI based on MetaCyc (d) and KEGG (e) databases. $P < 0.05$, *$P < 0.01$, **$P< 0.001$.

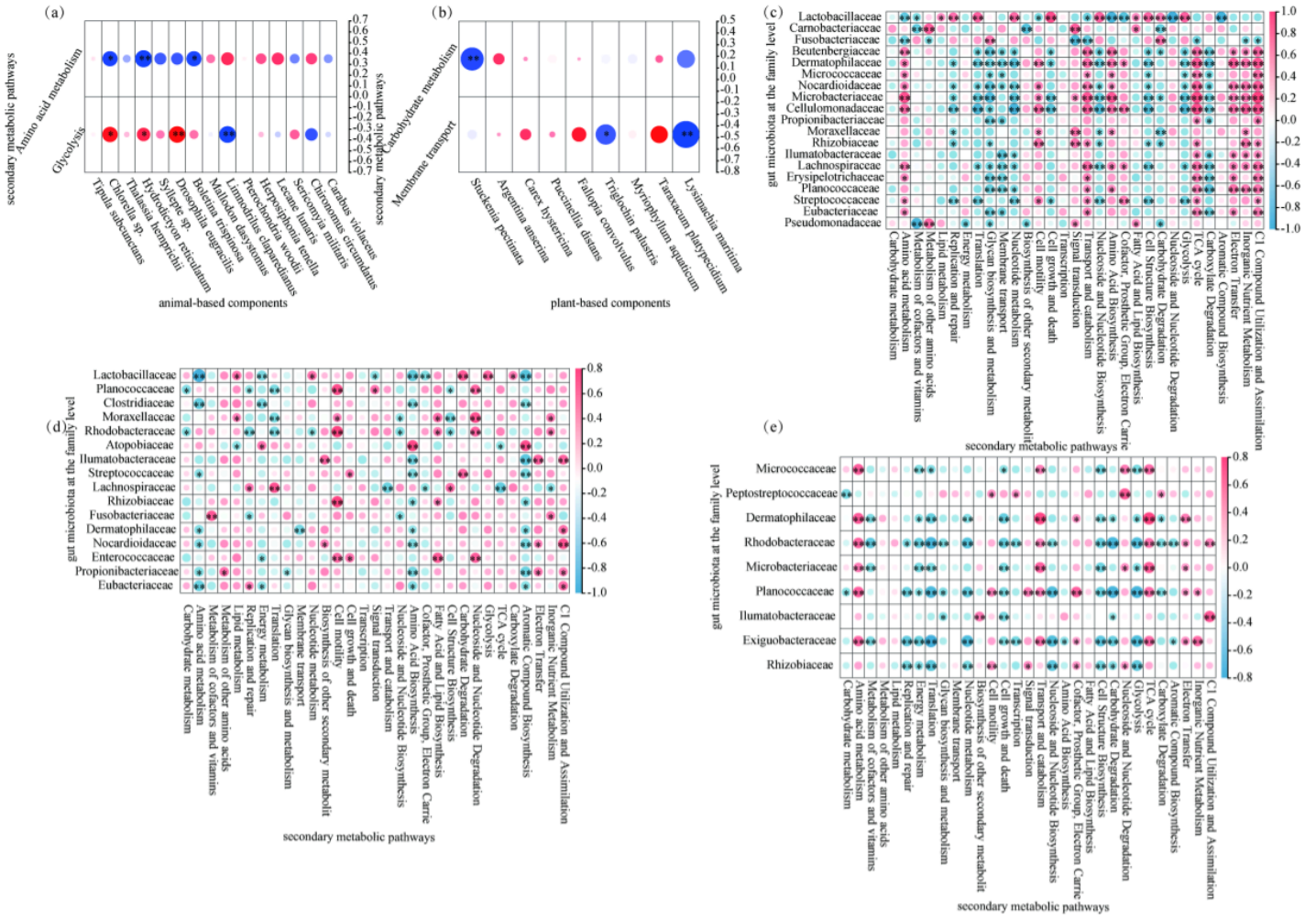

Figure 7

Spearman correlations between significantly different metabolic pathways and food components of *T. ferruginea* (a: animal- and plant-based) and plant-based components of *G. nigricollis* (b). Spearman correlations between family-level gut microbiota and significantly different metabolic pathways of *G. nigricollis* (c), *T. ferruginea* (d), and *A. indicus* (e).